Stock assessment of blue marlin (*Makaira nigricans*) in the Indian Ocean using Stock Synthesis

Wen-Qi Xu, Sheng-Ping Wang*, Chih-Yu Lin

Department of Environmental Biology and Fisheries Science, National Taiwan Ocean University, Keelung, Taiwan.
* Corresponding author: wsp@mail.ntou.edu.tw

Paper submitted to the 20th meeting of the Working Party on Billfish, Indian Ocean Tuna Commission, 12-15 September, 2022.

ABSTRACT

In this study, Stock Synthesis (SS) was applied to conduct the stock assessment for blue marlin in the Indian Ocean. The analyses were performed by incorporating historical catch, standardized CPUE series and length-frequency data. The results indicated that the estimated current stock status of blue marlin in the Indian Ocean varied depending on the assumptions related to natural mortality and the definition of fishing area. It should be noted that most of the life-history parameters used in this study were based on the values of blue marlin in the Pacific Ocean and this may lead to uncertainties in the evaluation of the stock status of blue marlin in the Indian Ocean.

1. INTRODUCTION

Blue marlin is largely considered to be a non-target species of industrial and artisanal fisheries. Longline catches account for around 68% of total catches in the Indian Ocean, followed by gillnets (15%), with remaining catches recorded under coastal longline, troll and handlines. Based on the catches data from 2015 to 2019, main fleets consisted of Taiwan (longline, 43%), Sri Lanka (gillnet, hook and line and longline, 21%), and Indonesia (longline, hook and line, 7%). Catches reported by drifting longliners were more or less stable until the late-70's, at around 3,000 t to 4,000 t, and have steadily increased since then to reach values between 8,000 t and to over 10,000 t since the early 1990's. The highest catches reported by longliners have been recorded since 2012, and are likely to be the consequence of higher catch rates by some longline fleets which appear to have resumed operations in the western tropical Indian

Ocean. (IOTC, 2018; IOTC, 2021a).

Since historical standardized CPUE and length-frequency data were available for blue marlin in the Indian Ocean, and parts of auxiliary information, such as life-history parameters, could be obtained from previous stock assessment for blue marlin in the other oceans, the integrated stock assessment approach can be applied to evaluate the stock status for blue marlin in the Indian Ocean. Therefore, this study attempt to conduct the stock assessment for blue marlin in the Indian Ocean using Stock Synthesis (SS, Methot, 2012; Methot and Wetzel, 2014).

2. MATERIALS AND METHODS

2.1 Fishery definition

Blue marlin was mainly exploited by longline fleets (Taiwan, Japan and Indonesia) and gillnet fleets (Pakistan, Iran, and Sri Lanka). However, the catch data and standardized CPUE series were only available for Taiwanese, Japanese and Indonesian fleets. For length-frequency data, long term data were only available for Taiwanese and Japanese fleets although the data were also available in recent years for some other fleets but the sample sizes were sparse for most of the years. Therefore, the fleets operated in the Indian Ocean were simply aggregated into the 4 fisheries (JPN: Japanese longline; TWN: Taiwanese longline; IDN: Indonesian longline; OTH: Other fleets).

In addition, the previous meetings suggested that the relative abundance indices and size compositions may be varied by areas. In this study, a two-area definition (west and east), following the area definition of nominal catch provided by IOTC, was also used to separate Japanese, Taiwanese and other fleets by areas (JPN_W, JPN_E, TWN_W, TWN_E, OTH_W and OTH_E).

2.2 Data used

The historical catches in weight and length-frequency data for all fleets were provided by Indian Ocean Tuna Commission (IOTC). Fig. 1 shows the trends of catches for fours fisheries. The total catch obviously increased since early 1990s and the increase in catch mainly contributed from OTH and TWN.

The relative abundance indices used in this study were based on the standardized CPUE of Taiwanese, Japanese and Indonesian longline fleets (Lin et al., 2022; Matsumoto et al., 2022; Setyadji et al., 2022). In addition, the standardized CPUE of

Taiwanese and Japanese fleets were conducted by areas (Fig. 2) and thus the assessment models were derived by incorporating different combinations of the standardized CPUE series. However, as the suggestion of WPTT (IOTC, 2021b), Taiwanese data before 2005 were recommended not using to analyze the targeting of fishing operations and conduct the CPUE standardization for tropical tunas due to the problem of data quality. Therefore, updated Taiwanese standardized CPUE data were available from 2005 to 2020, while the historical CPUE data of 1979-2004 were obtained from the previous assessment (Wang, 2019). Japanese standardized CPUE data were available from 1979 to 2010 for area NW and from 1979 to 2020. Indonesian standardized CPUE data were from 2006 to 2020.

The length data of blue marlin in the Indian Ocean were mainly collected by Japanese and Taiwanese longline fleets. Although the data also collected by other fleets, such as Korea, Sri Lanka, EU countries and China, the time series of the data were generally short or incomplete. All of the length-frequency data were converted into the measurement of eye fork length (EFL) and aggregated into 3 cm length interval (Fig. 3).

Fig. 4 shows the data presence by year for each fleet used in the stock assessment of blue marlin in the Indian Ocean, including catch, length-frequency and CPUE data.

2.3. Life-history parameters

Because the life-history parameters are still not available for blue marlin in the Indian Ocean, the assessment models were performed using the same parameters adopted in the previous assessment (Wang, 2019).

Growth of blue marlin has been known to be sexual dimorphic and females grow faster than males (Fig. 5) (e.g. Lee et al., 2013; 2014). SS provides three growth models as options, including von Bertalanffy growth curve, Schnute's generalized growth curve (aka Richards curve) and von Bertalanffy growth curve with age-specific deviations for growth coefficient (K). In this study, the standard von Bertalanffy growth curve was used and it was parameterized as:

$$L_2 = L_\infty + (L_1 - L_\infty)e^{-K(A_2 - A_1)}$$

where L_1 and L_2 are the sizes associated with ages near the youngest A_1 and oldest A_2 ages in the data, K is the growth coefficient, and L_∞ is the theoretical maximum length which can be solved based on the values other three parameters. In this study, growth parameters were fixed to those adopted by Lee et al. (2013, 2014) for the assessment of blue marlin in the Pacific Ocean.

Setyadji et al. (2014) provided a relationship for blue marlin in the Indian. However, EFL data can be converted into unreasonable high weights for fishes with large lengths when the relationship of Setyadji et al. (2014) was used. Therefore, the length-weight relationship of Lee et al. (2013, 2014) was adopted as the use of the previous assessment.

There is little information about natural mortality (M) for blue marlin in the Indian Ocean. Lee et al. (2013, 2014) used sex- and age-specific natural mortality for the assessment of blue marlin in the Pacific Ocean. Based on the age-specific natural mortality used in Lee et al. (2013, 2014), the values were fixed as 0.42 year^{-1} for age 0, 0.37 year^{-1} for age 1, 0.32 year^{-1} for age 2, 0.27 year^{-1} for age 3, and 0.22 year^{-1} for age above 4 for female and 0.42 year^{-1} for age 0, 0.37 year^{-1} for age above 1 for male. As the previous assessment, the values for adult fishes (0.22 year^{-1} for females and 0.37 year^{-1} for males) were used for the assessment of blue marlin in the Indian Ocean as a reference case. In addition, Lorenzo parameterization was also used to calculate age-specific natural mortalities for females and males based on the parameters of growth function and length-weight relationship (Fig. 6).

The maturity ogive of blue marlin in the western Pacific Ocean (Sun et al., 2009) was used in this study. The value of length at 50% maturity was 179.76 cm and slope of the logistic function was -0.2039.

The standard Beverton-Holt stock-recruitment relationship was used in this study. There is also little information about the parameters of the stock-recruitment relationship (steepness, *h*), which represented the productivity of the fish. Therefore, the assumption used in Lee et al. (2013, 2014) was adopted in this study and value of *h* was assumed to be 0.87.

The values of life-history parameters used in this study are listed in Table 1 and these values were used as the base-case.

2.4 Model structure and assumption

Stock Synthesis (SS) version 3.30.19 (Methot et al., 2022) was used in this study. Equal weightings were assigned to all data components.

The population structure was sex-specific although sex specific data were not available but the model population age structure can be differentiated by sexes. The maximum age used in the model was 40 years. The time period of assessment model was from 1950 to 2020 along with 10-years projection. Sex ratio of female was assumed to be 0.5.

Recruitment was estimated as deviates from the Beverton-Holt stock recruitment relationship and was assumed to follow a lognormal distributed deviates with zero mean and standard deviation (σ_R). In this study, the σ_R was assumed to be 0.4, which was commonly adopted in previous stock assessment for tunas and billfishes. Recruitment deviations were assigned and estimated for 1970-2020 in the model and deviates for other years were fixed at zero.

Selectivity curves were length-based and modeled using double normal functions because the length-frequency compositions tended to concentrate at specific ranges for fleets. In addition, selectivity was time-invariant for all fleets. Due to the incomplete time-series or insufficient sample sizes for the length-frequency data of IDN and OTH, the selectivities of IDN and OTH were assumed to be the same with TWN.

Catchability was estimated assuming that survey indices are proportional to vulnerable biomass with a scaling factor of catchability. It was assumed that catchability was constant over time for all indices (Lee et al. 2013).

As Methot (2012) recommended in most cases, fishing mortality (F) was modelled the method of a hybrid F method that does a Pope's approximation to provide initial values for iterative adjustment of the Baranov continuous F values to closely approximate the observed catch.

2.5 Diagnostics and retrospective analysis

The residual diagnostics of the model fits to the data and the retrospective analysis were using the functions of R package "ss3diags" (Carvalho et al., 2021). In addition, the package was also implemented based on a delta-multivariate lognormal approximation to generate joint error distributions for the relative spawning biomass and fishing mortality to the reference point MSY.

2.6 Scenarios

The standardized CPUE series revealed different patterns by fleets and areas although the trends may be relatively similar within fleets (Fig. 2). To include all of possible information on the relative trend of abundance, the standardized CPUE series of Taiwanese, Japanese and Indonesian fleets were all adopted for the assessment models and the models were derived by incorporating different combinations of standardized CPUE series (Table 2).

Based on the life-historical parameters and assumption and structure of the model, various scenarios were also created to examine the model estimated stock status when different input data were used.

S0: the same data and model specification with the scenario “S7” adopted in the previous assessment;

S1: the same model specification with S0 and all data updated (Taiwanese CPUE data of 1979-2004 were obtained and used from the previous assessment);

S2: as S1 but Japanese and Taiwanese fleets and their catch and length-frequency data were separated by areas;

S3: as S1 but age-specific natural mortalities were used;

S4: as S2 but age-specific natural mortalities were used;

S5~S8: repeat S1~S4 but Taiwanese CPUE data of 1979-2004 were excluded.

2.7 Scenarios suggested by WPB

S9: as S6 but selectivity of IDN assumed to be the same with JPN_E;

S10: as S8 but the mean values of age-specific natural mortalities were scaled to the same as fixed natural mortality (Fig. 6).

3. RESULTS AND DISCUSSIONS

3.1. Model fits and diagnostics

Generally, the models can well fit the trends of TWN and JPN CPUE series under all scenarios although they provided different fits to each data point (Fig. 7). The mode fits and Pearson residuals plots for the length-frequency data were shown in Figs. 3 and 8. Pearson residuals plots were illustrated for S1 and S2 as examples and similar results were observed for other scenarios. The results indicated that the relatively poor model fits for the length-frequency data for TWN before the early 2000s, when more small fishes were caught but the models cannot well fit the distribution patterns. The model fits also deteriorated for JPN after the early 2000s due to the sparse sample sizes (Figs. 3 and 8). However, the problem in the model fits of length-frequency data cannot be determined by the comparison between TWN and JPN data because most of the catches caught by JPN were larger than 100 cm.

The run test and joint residual plots obtained from all scenarios were shown in Figs. 9 and 10. The results indicated the residuals from most CPUE data did not fit the hypothesis of random distribution but revealed patterns with time for most scenarios, except for JPN_CE and IDN, while the assumption of age-specific natural mortality can improve the residual pattern for TWN_NE. RMSE also revealed relatively low precisions for the model fits of CPUE data (RMSE > 20 %). In addition, the residuals of the length-frequency data did not randomly distribute, except for JPN or JPN_W, while RMSE were 6.4-6.8% for all scenarios.

3.2. Model estimates

The model estimated selectivity curves by scenarios are shown in Fig. 11. TWN obviously tended to select the smaller fishes than those of JPN, while JPN tended to select large fishes with a wide range of body size. In addition, Japanese selectivity curves were changed from asymptotic looks to dome-shaped when age-specific natural mortality was assumed.

Time trajectories of the model-estimated recruitment, spawning biomass and fishing mortality were shown in Fig. 12. The estimates of recruitment in this study were obviously lower than those of the previous assessment and similar trends were observed for all scenarios after the 1990s. The estimates of spawning biomass and fishing mortality revealed diverse patterns depending on the assumption of natural mortality. The estimates obtained based on the assumption of age-specific natural mortality (S3, S4, S7 and S8) resulted in much higher spawning biomass and lower fishing mortality than those based on fixed natural mortalities (S1, S2, S5, S6, S9 and S10). Spawning biomass obviously declined from the mid-1990s to 2010 because of a substantial increase in catches. For the scenarios of fixed natural mortalities (S1, S2, S5, S6, S9 and S10), spawning biomass slightly increased from the late 2000s to the mid-2010s and this might result from the strong recruitment and reduction in fishing mortality after the late 2000s. However, spawning biomass continuously decreased when the assumption of age-specific natural mortality was used (S3, S4, S7 and S8). In recent years, the recruitment and spawning biomass revealed continuous decreasing trends since fishing mortality remained at a relatively high level.

Time trajectories of the relative fishing mortality and relative spawning biomass indicated that the recent spawning biomass was lower than the MSY level and less 40% of its unfished level, and the fishing mortality also exceed the MSY level after the mid-2000s from scenarios of fixed natural mortalities (S1, S2, S5, S6, S9 and S10), while spawning biomass remained at a relatively high level and fishing mortality was also still lower than the MSY level from the assumption of age-specific natural mortality (S3, S4, S7 and S8) (Fig. 13).

Fig. 14 shows the Kobe plot based on the estimates obtained from various scenarios. Overall, the results of most scenarios indicated that the current stock status of blue marlin in the Indian Ocean was not overfished and not overfishing, but it may be subject to overfishing and overfished when fixed natural mortality and two-area assumptions were used (S2, S6, S9 and S10). The Kobe plot obtained from the selected scenario (S10) were shown in Fig. 15.

Table 3 shows the model estimates of the key management quantities obtained from various scenarios. According to the results from parallel scenarios with the exclusion of historical Taiwanese CPUE data (S1 correspond to S5, S2 corresponds to S6 and so on), the model estimates were not significantly affected when removing the historical Taiwanese CPUE series. The estimates of key quantities of management interests obtained from the selected scenario (S10) were shown in Table 4. Kobe II Strategy Matrix, including the probability of exceeding the MSY-based target reference points and achieving the green quadrant of the Kobe plot under the constant catch with 10-110% of the 2020 catch level (7,126 t) for 10 years projection, were shown in Tables 5 and 6. In order to achieve the Commission objectives of being in the green zone of the Kobe plot by 2027 with at least a 60% chance, the catches of blue marlin would have to be reduced by 10% compared to the 2020 catch.

REFERENCE

Carvalho, F., Winker, H., Courtney, D., Kapur, M., Kell, L., Cardinale, M., Schirripag, M., Kitakado, T., Yemane, D., Piner, K.R., Maunder, M.N., Taylor, I., Wetzel, C.R., Doering, K., Johnsonm, K.F., Methot, R.D., 2021. A Cookbook for Using Model Diagnostics in Integrated Stock Assessments. Fish. Res. 240: 105959.

IOTC, 2018. Report of the 16th Session of the IOTC Working Party on Billfish. IOTC-2018-WPB16-R[E].

IOTC, 2021a. Report of the 19th Session of the IOTC Working Party on Billfish. IOTC-2021-WPB19-R[E].

IOTC, 2021b. Report of the 23rd Session of the IOTC Working Party on Tropical Tunas, Data Preparatory Meeting. IOTC-2021-WPTT23(DP)-R[E].

Lee, H.H, Chang, Y.J, Hinton, M.G., Piner, K.R., Tagami, D., Taylor, I., Kai, M., 2013. Blue marlin (*Makaira nigricans*) stock assessment in the Pacific Ocean.

ISC/13/BILLWG-2/04.

Lee, H.H., Piner, K.R., Methot Jr., R.D., Maunder, M.N., 2014. Use of likelihood profiling over a global scaling parameter to structure the population dynamics model: An example using blue marlin in the Pacific Ocean. Fish. Res. 158: 138-146.

Lin, C.Y., Wang, S.P., Xu, W.Q., 2022. CPUE standardization of blue marlin caught by Taiwanese large scale longline fishery in the Indian Ocean. IOTC–2022–WPB20–09.

Matsumoto, T., Taki, K., Ijima, H., 2022. Standardized CPUE of blue marlin (*Makaira mazara*) caught by Japanese longline fishery in the Indian Ocean: Analysis between 1979 and 2021. IOTC-2022-WPB20-10.

Methot R.D., Wetzel, C.R., 2014. Stock synthesis: A biological and statistical framework for fish stock assessment and fishery management. Fish. Res. 142: 86-99.

Methot, R.D., 2012. User manual for Stock Synthesis. NOAA Fisheries, Seattle, WA.

Methot. R.D., Wetzel, C.R., Taylor, I.G., Doering, K.L., Johnson, K.F., 2022. Stock Synthesis User Manual, version 3.30.19. NOAA Fisheries, Seattle, WA.

Setyadji, B., Jatmiko, I., Wujdi, I., Nugraha, B., 2014. Preliminary analysis of length – weight relationship of swordfish (*Xiphias gladius*), black marlin (*Makaira indica*), and blue marlin (*Makaira nigricans*) caught by Indonesian longliners in the Indian Ocean. IOTC–2014–WPB12–13

Setyadji, B., Parker, D., Wang, S.P., 2022. Update on CPUE Standardization of Blue Marlin (*Makaira nigricans*) from Indonesian Tuna Longline Fleets 2006-2021. IOTC–2022–WPB20–11.

Sun, C.L., Chang, Y.J., Tszeng, C.C., Yeh, S.Z., Su, N.J. 2009. Reproductive biology of blue marlin (*Makaira nigricans*) in the western Pacific Ocean. Fish. Bull. 107: 420-432.

Wang, S.P., 2019. Stock assessment of blue marlin in the Indian Ocean using Stock Synthesis. IOTC–2019–WPB17–21.

4 fleets

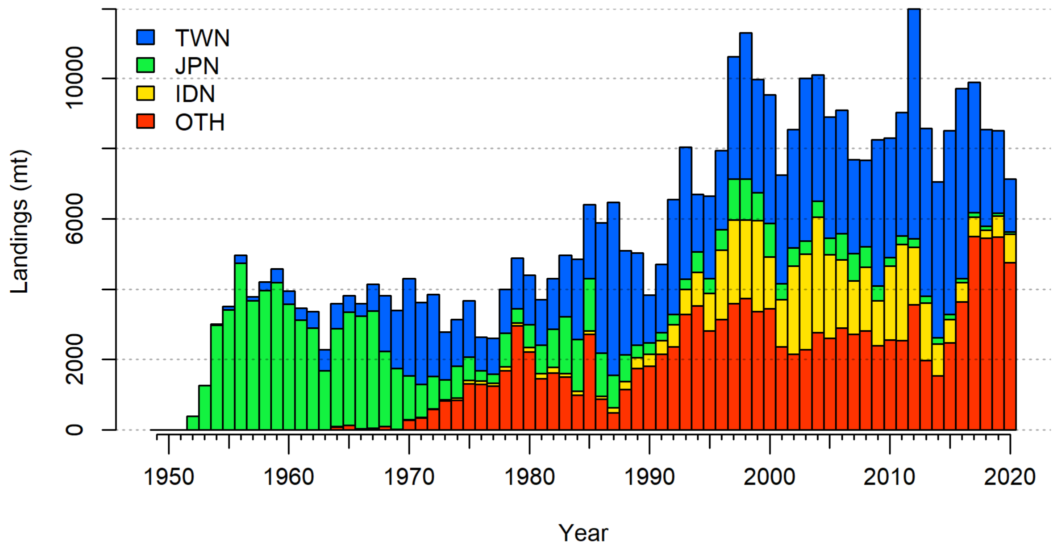

Separate Japanese, Taiwanese and other fleets by areas

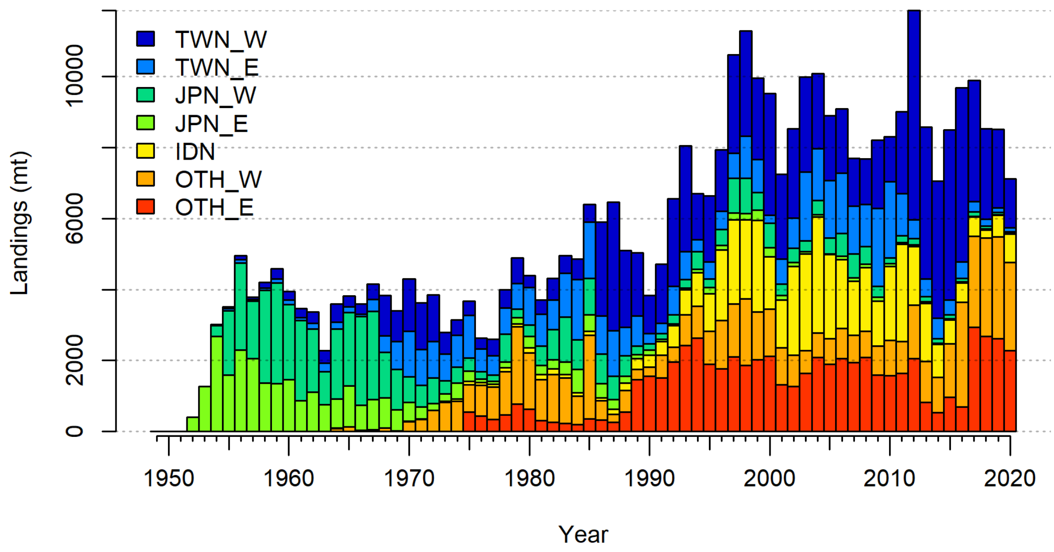

Fig. 1. Annual catches of blue marlin in the Indian Ocean by fleets.

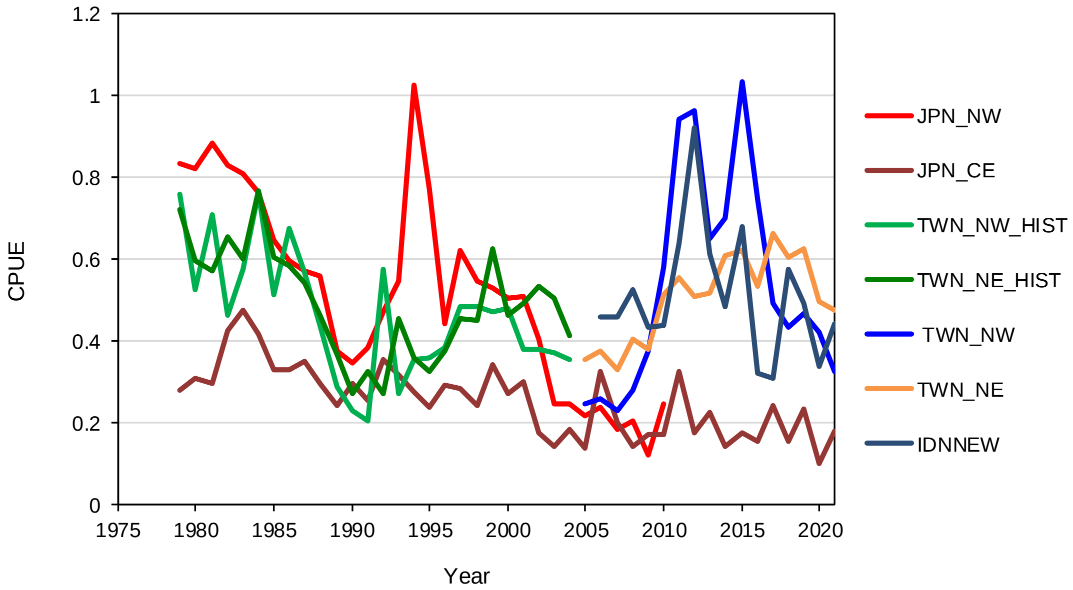

Fig. 2. Standardized CPUE series by fleets and areas used for the stock assessment of blue marlin in the Indian Ocean.

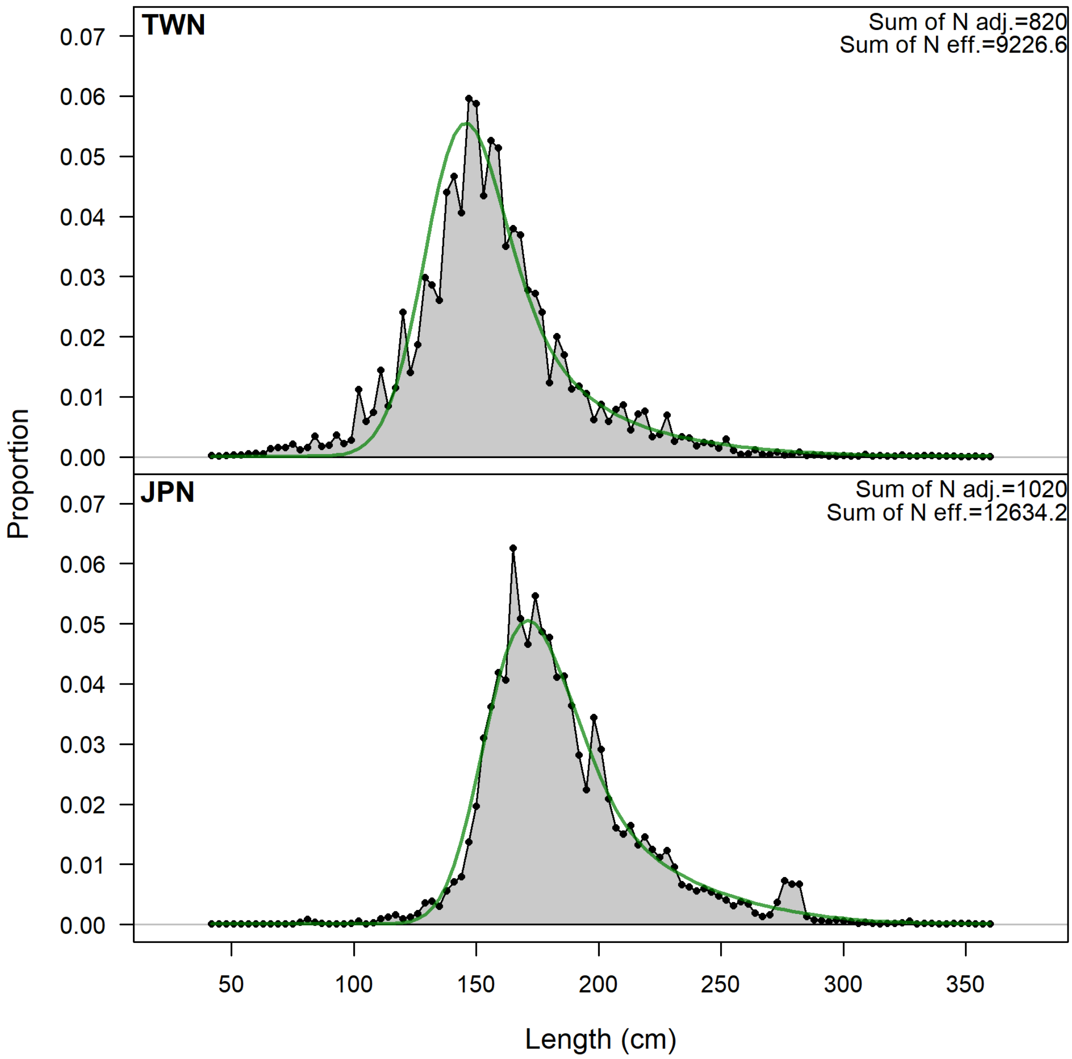

Fig. 3. Observed length-frequency aggregated across years of blue marlin in the Indian Ocean (predicted values were obtained from scenario "S1").

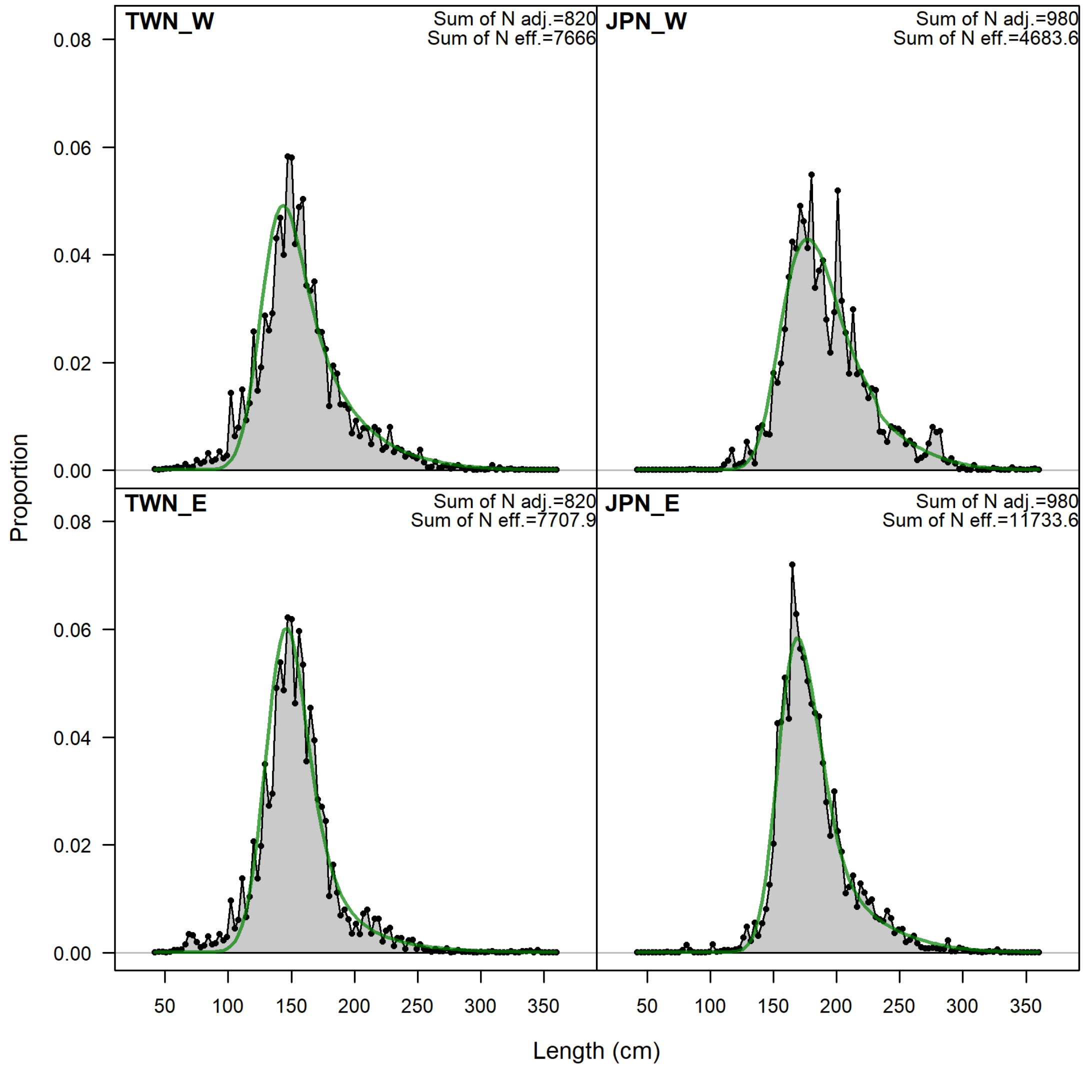

Fig. 3. (continued, predicted values were obtained from scenario “S2”).

4 fleets

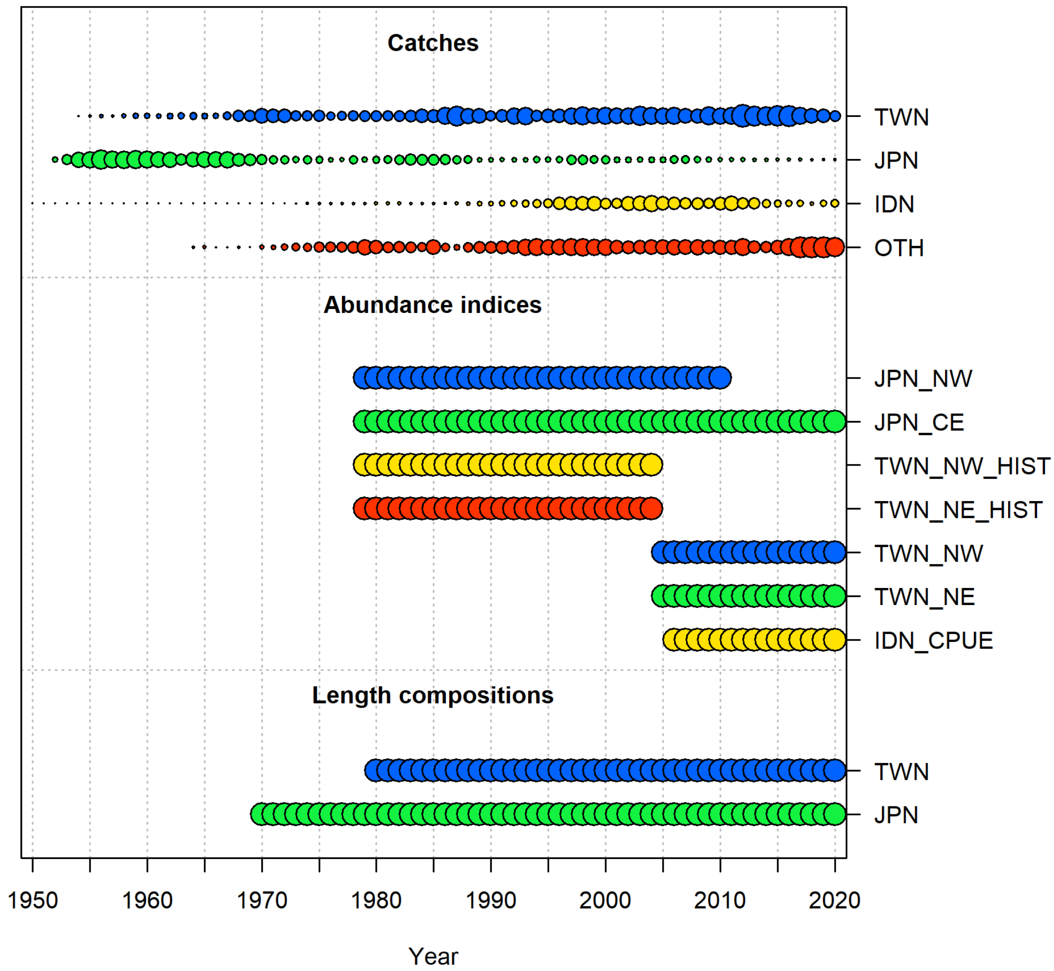

Fig. 4. Data presence by year for each fleet used for the stock assessment of blue marlin in the Indian Ocean.

Separate Japanese and Taiwanese fleets by areas

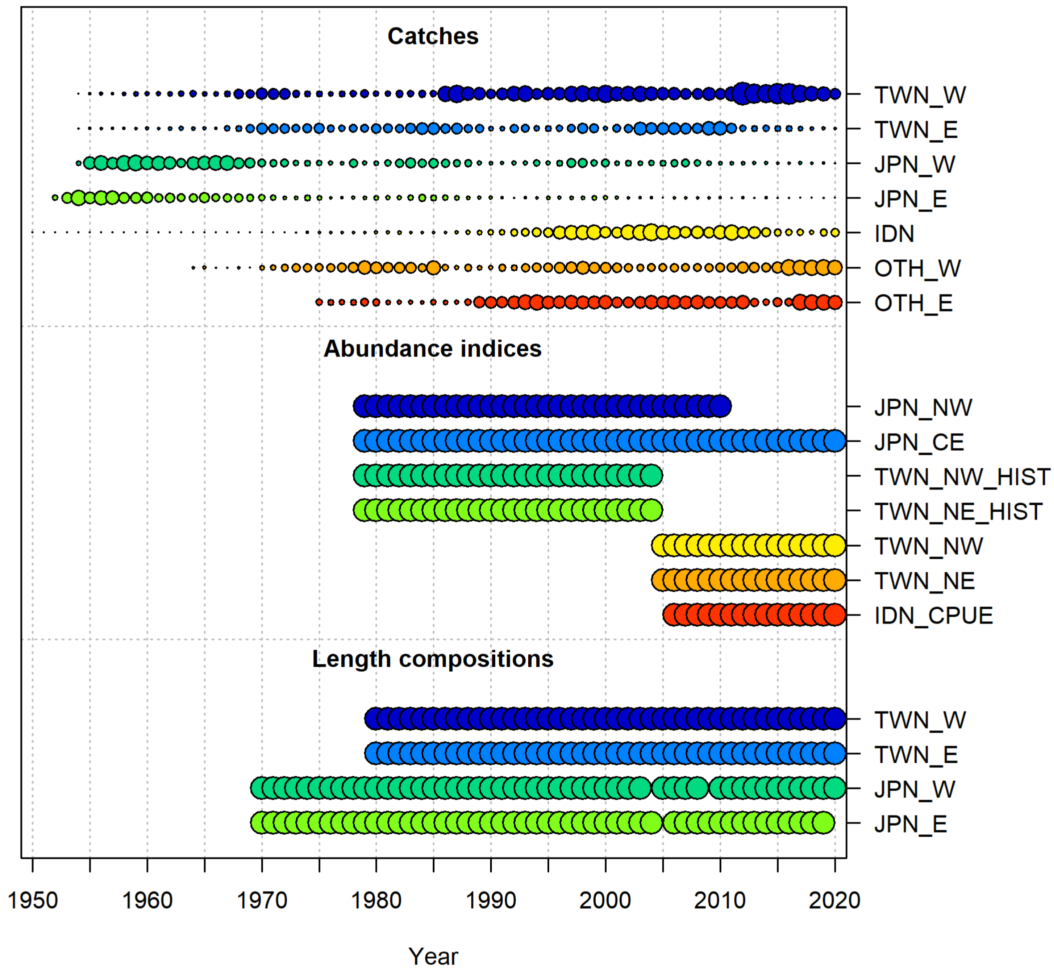

Fig. 4. (Continued).

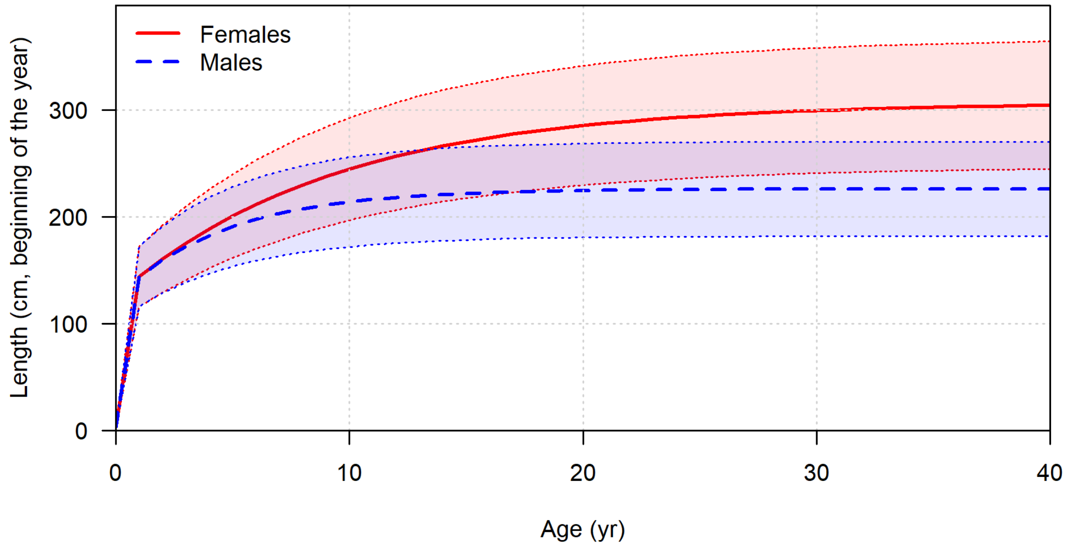

Fig. 5. Growth curves of blue marlin in the Indian Ocean.

(A)

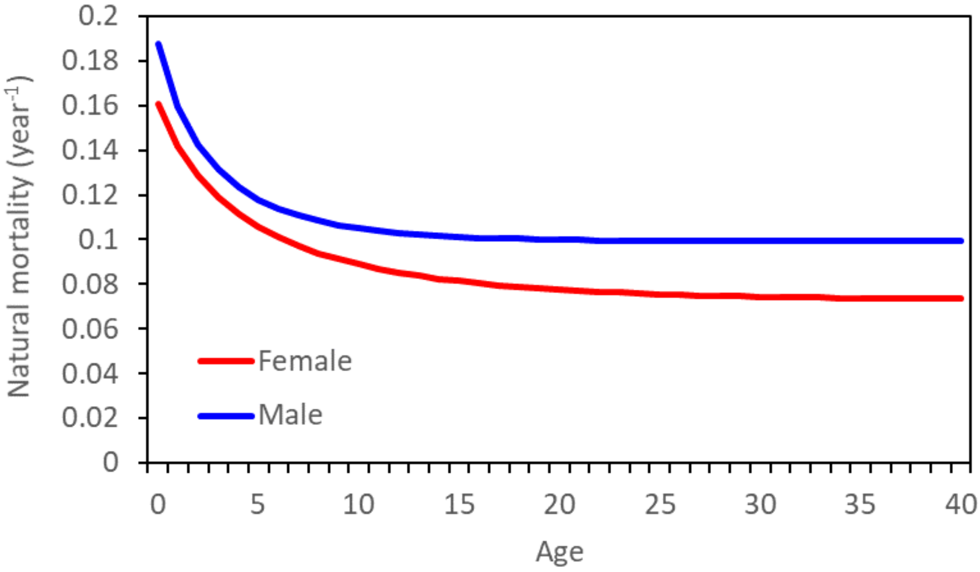

(B)

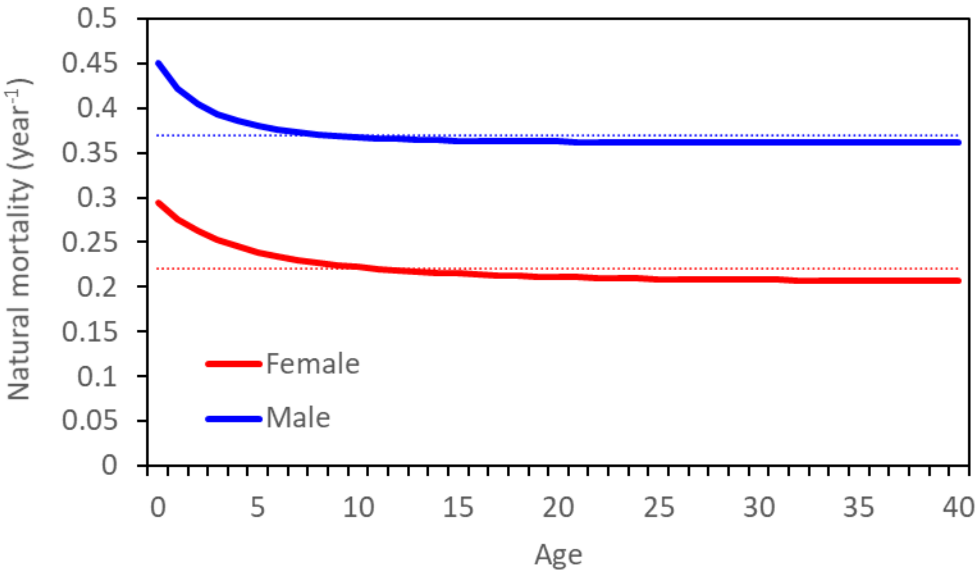

Fig. 6. Age-specific natural mortality for blue marlin in the Indian Ocean (A) and the mean values of age-specific natural mortalities scaled to the same as fixed natural mortality (B).

TWN_NW_HIST

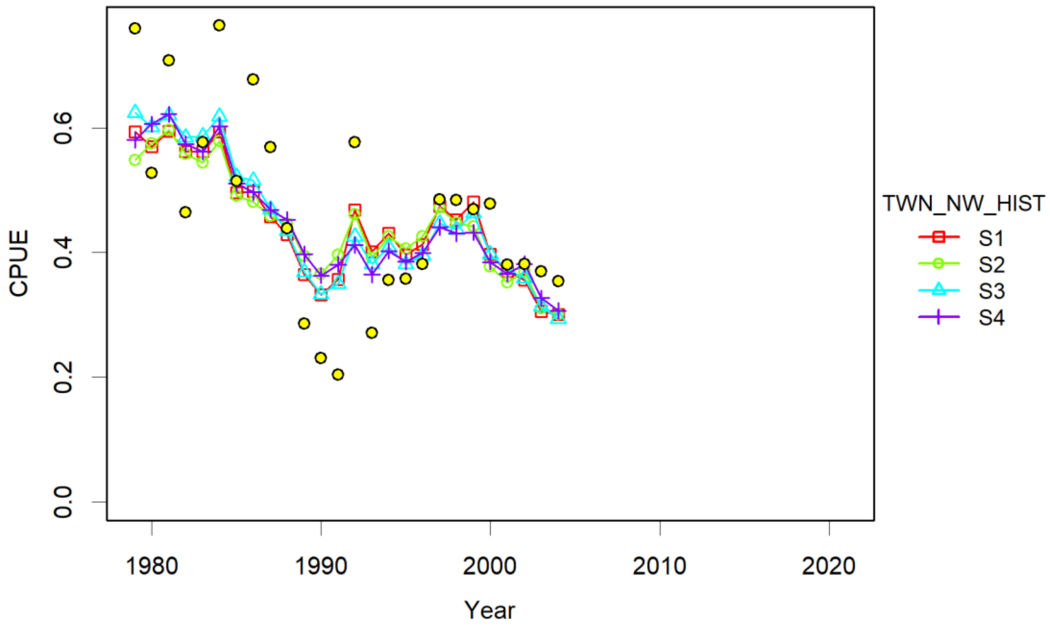

TWN_NE_HIST

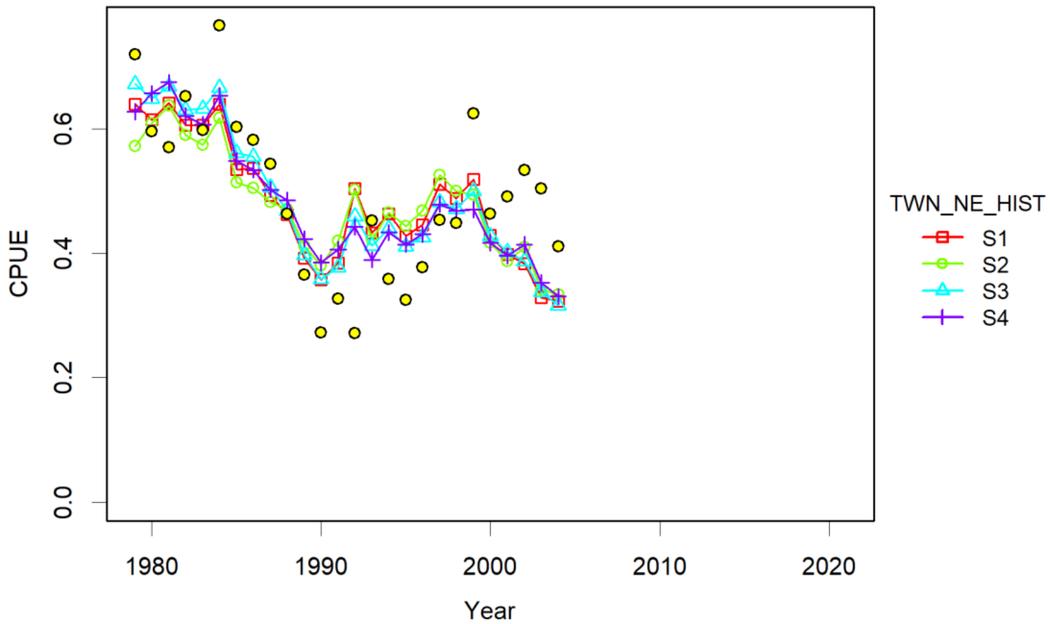

Fig. 7. Observed CPUE (dots) and model-estimated CPUE (lines) of blue marlin in the Indian Ocean.

TWN_NW

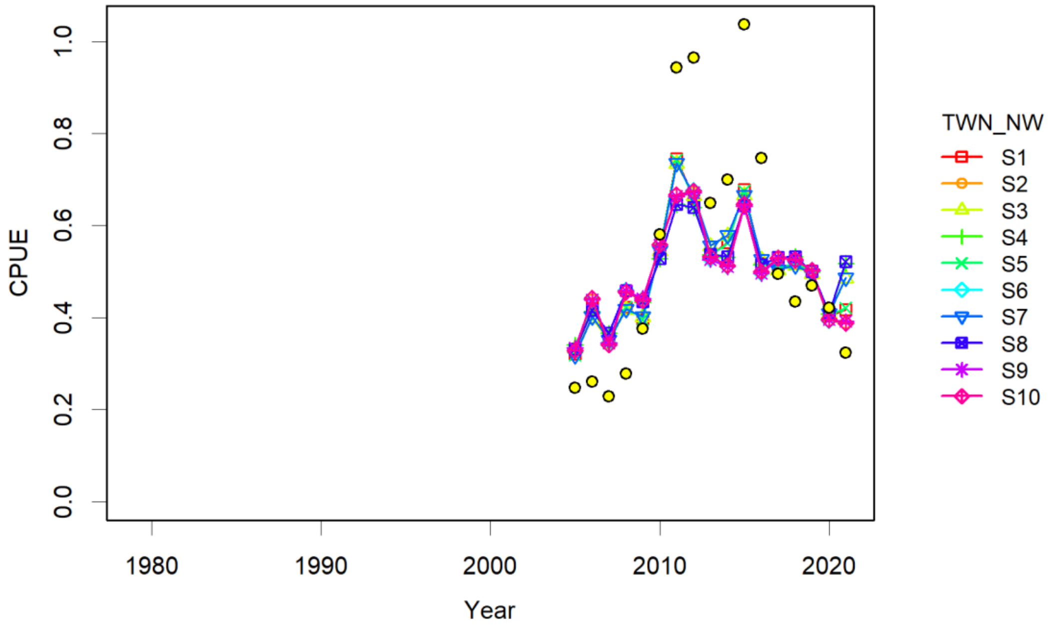

TWN_NE

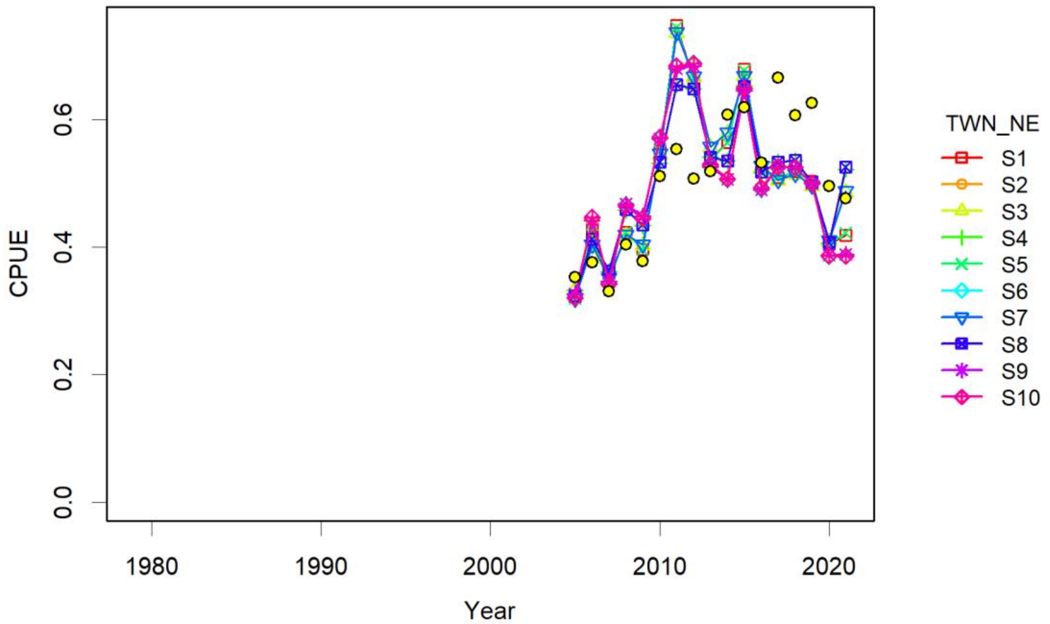

Fig. 7. (Continued).

JPN_NW

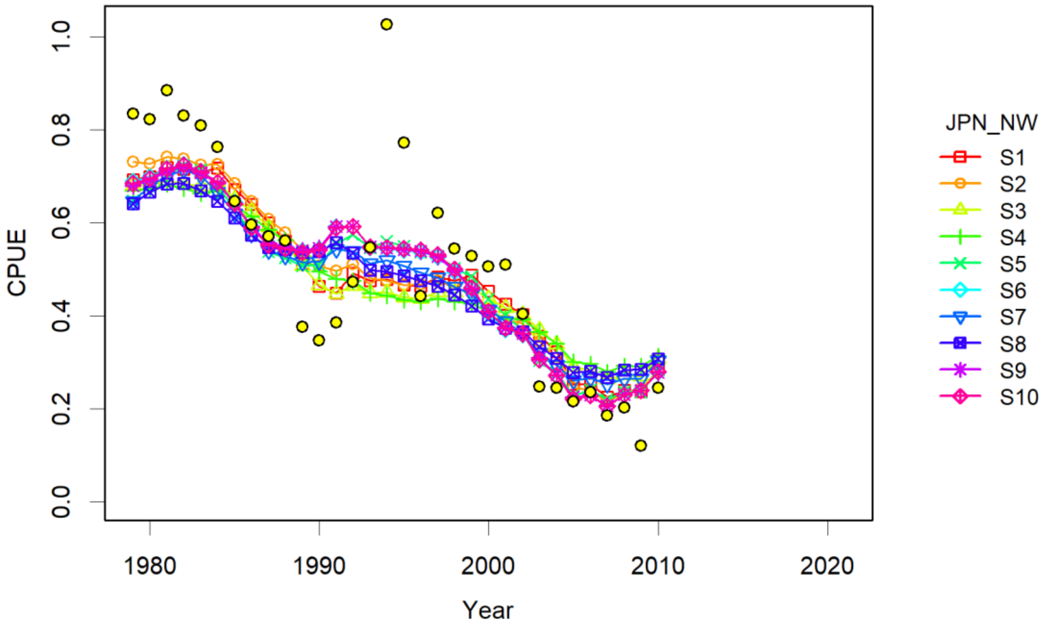

JPN_CE

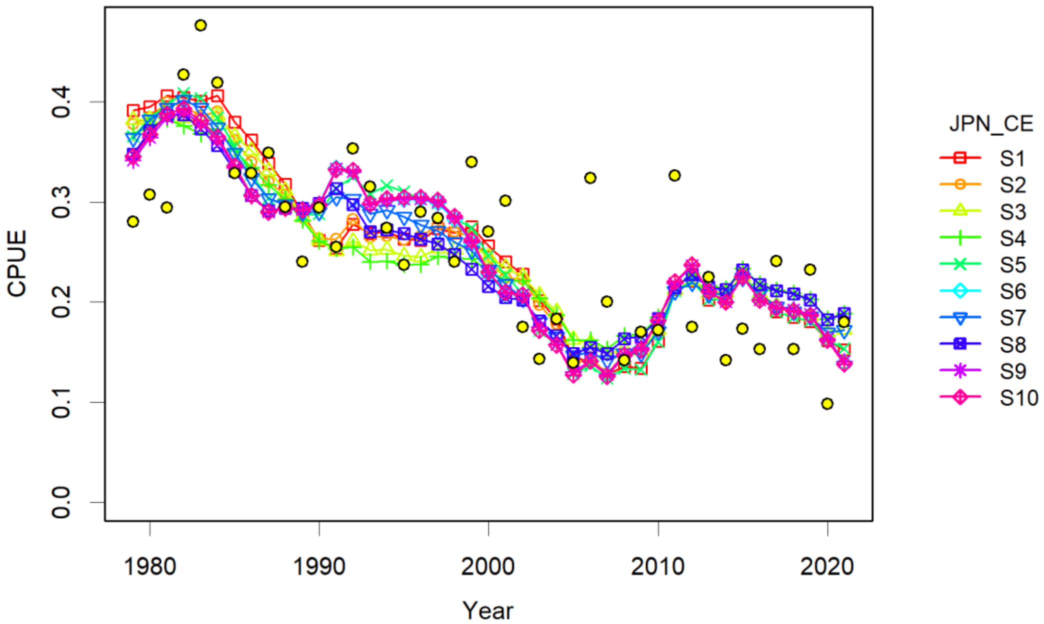

Fig. 7. (Continued).

IDN

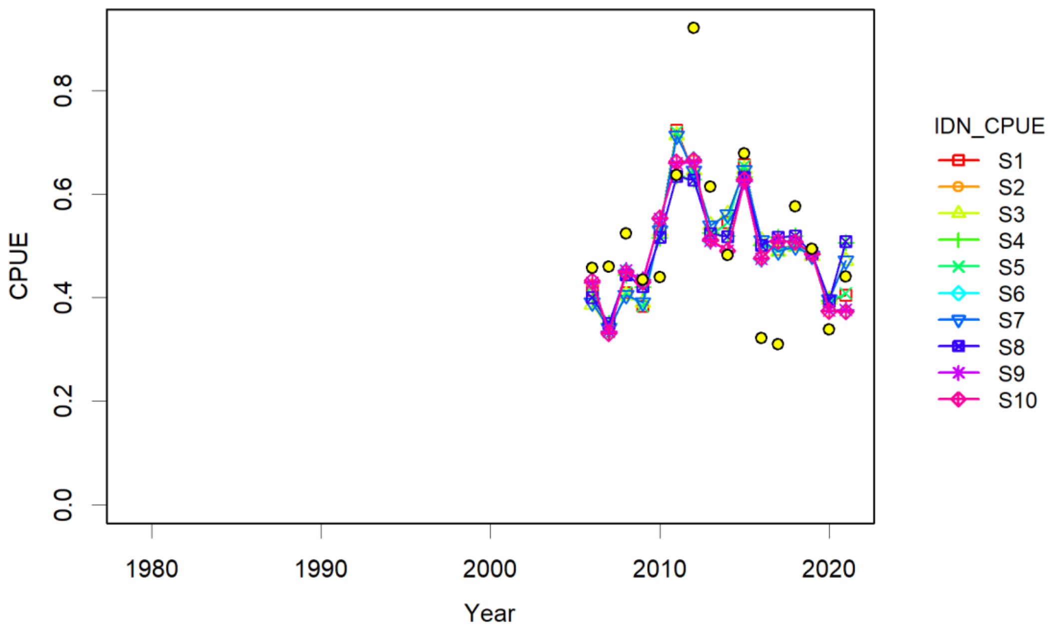

Fig. 7. (Continued).

Scenario “S1”

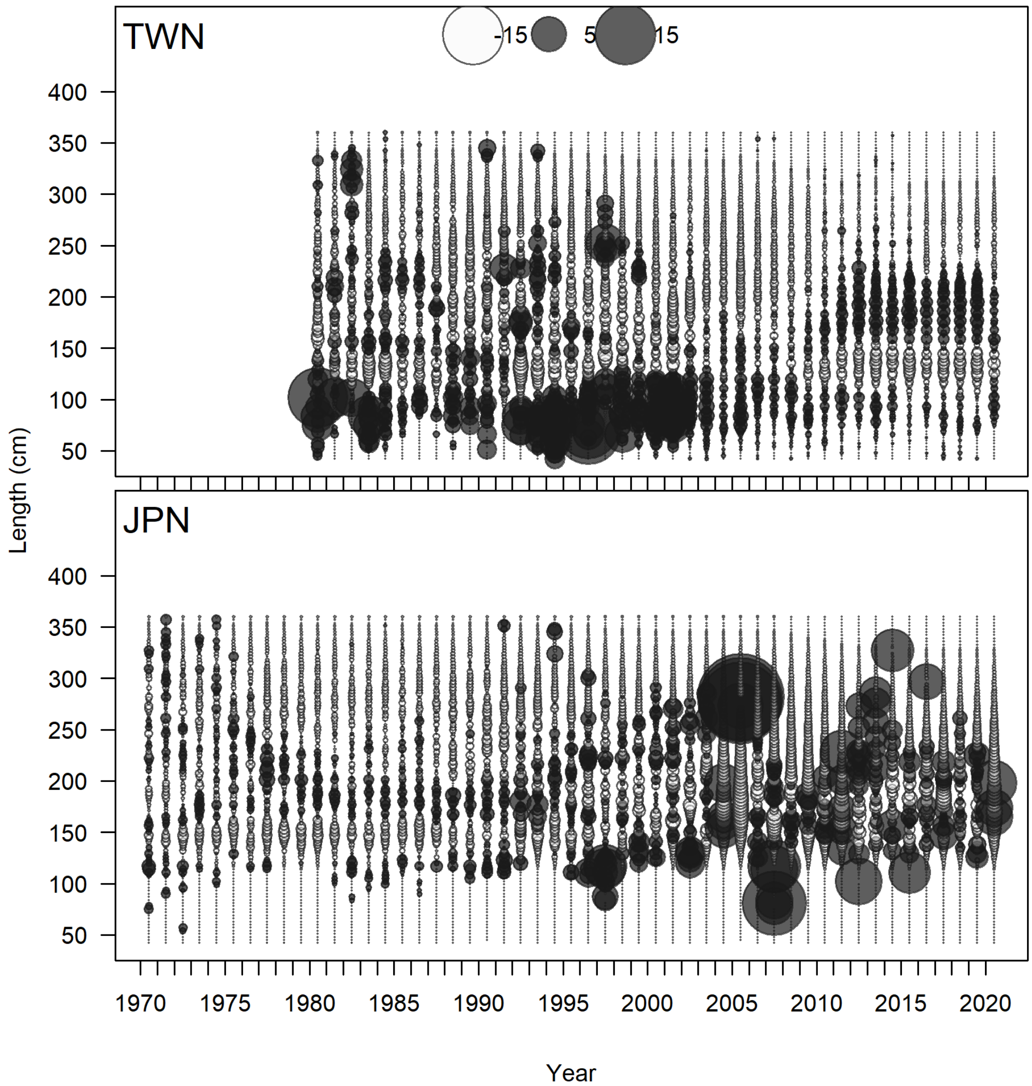

Fig. 8. Pearson residuals of the model fits to length-frequency data of blue marlin in the Indian Ocean. Closed bubbles are positive residuals (observed > expected) and open bubbles are negative residuals (observed < expected).

Scenario "S2"

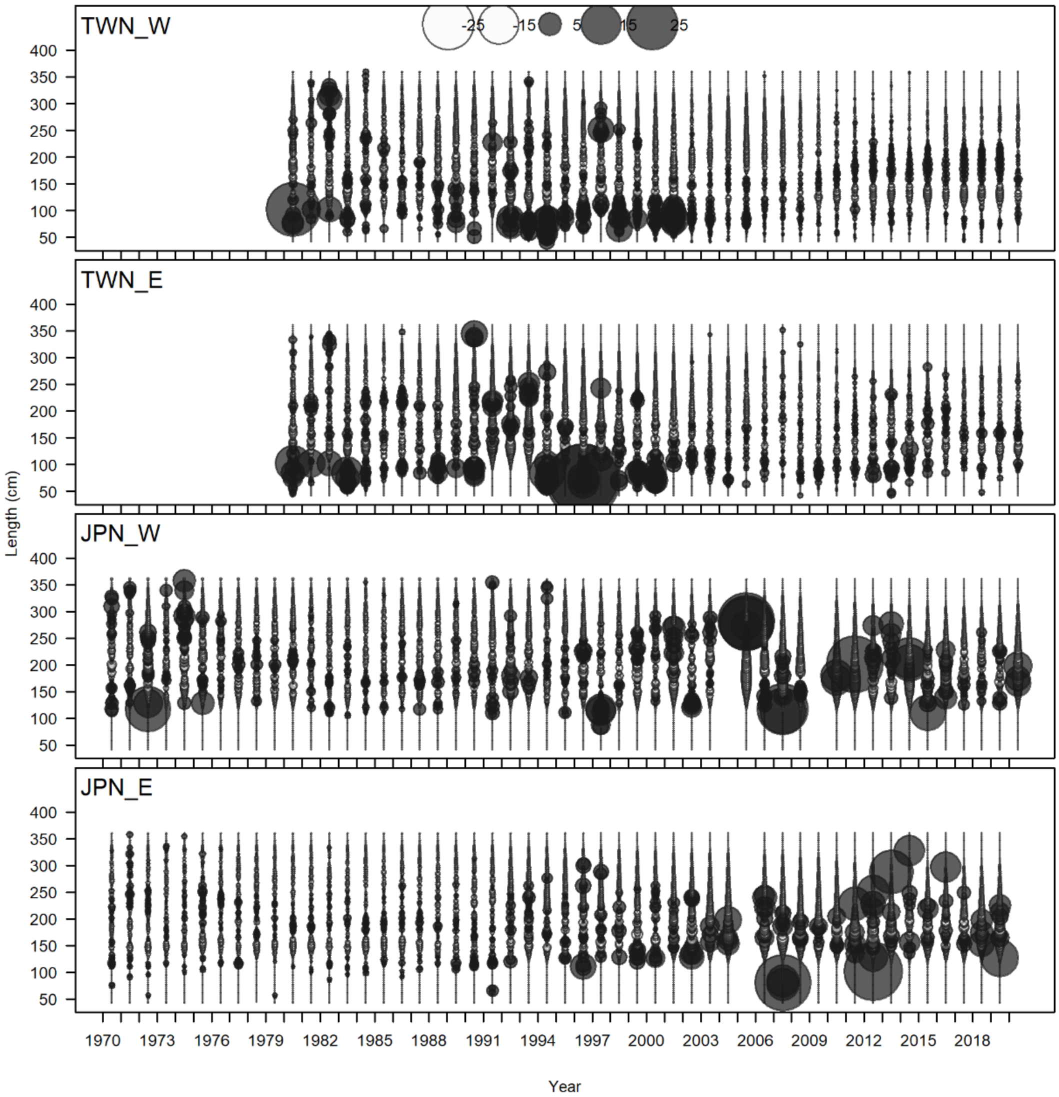

Fig. 8. (Continued).

Scenario "S1"

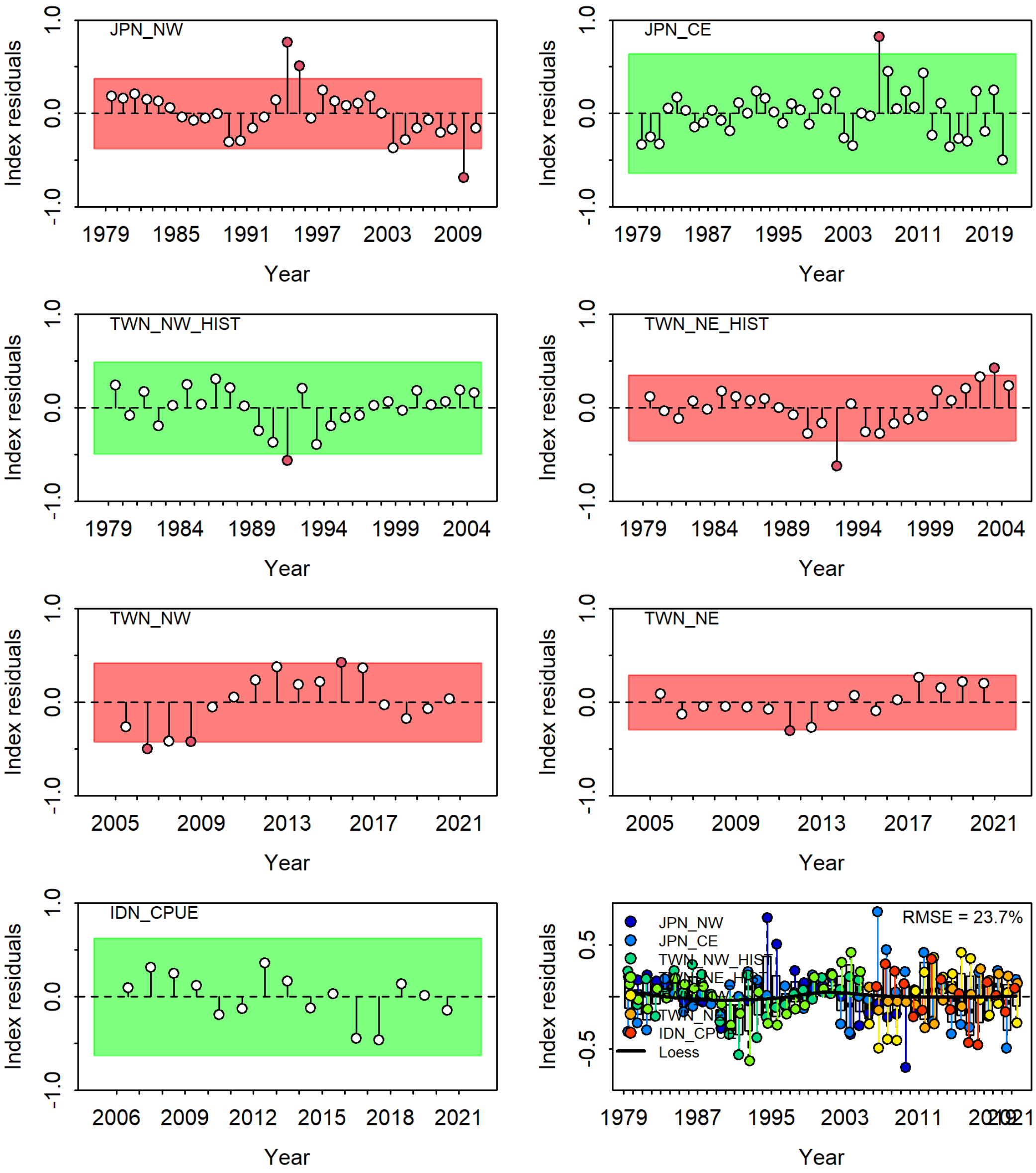

Fig. 9. Runs test plot (green shading indicates no evidence ($p \geq 0.05$) and red shading evidence ($p < 0.05$) to reject the hypothesis of a randomly distributed time-series of residuals, respectively) and Joint residual plot for fits to CPUE indices (vertical lines with points show the residuals, and solid black lines show loess smoother through all residuals, boxplots indicate the median and quantiles in cases where residuals from the multiple indices are available for any given year and root mean squared errors (RMSE) are included in the upper right-hand corner of each plot).

Scenario "S2"

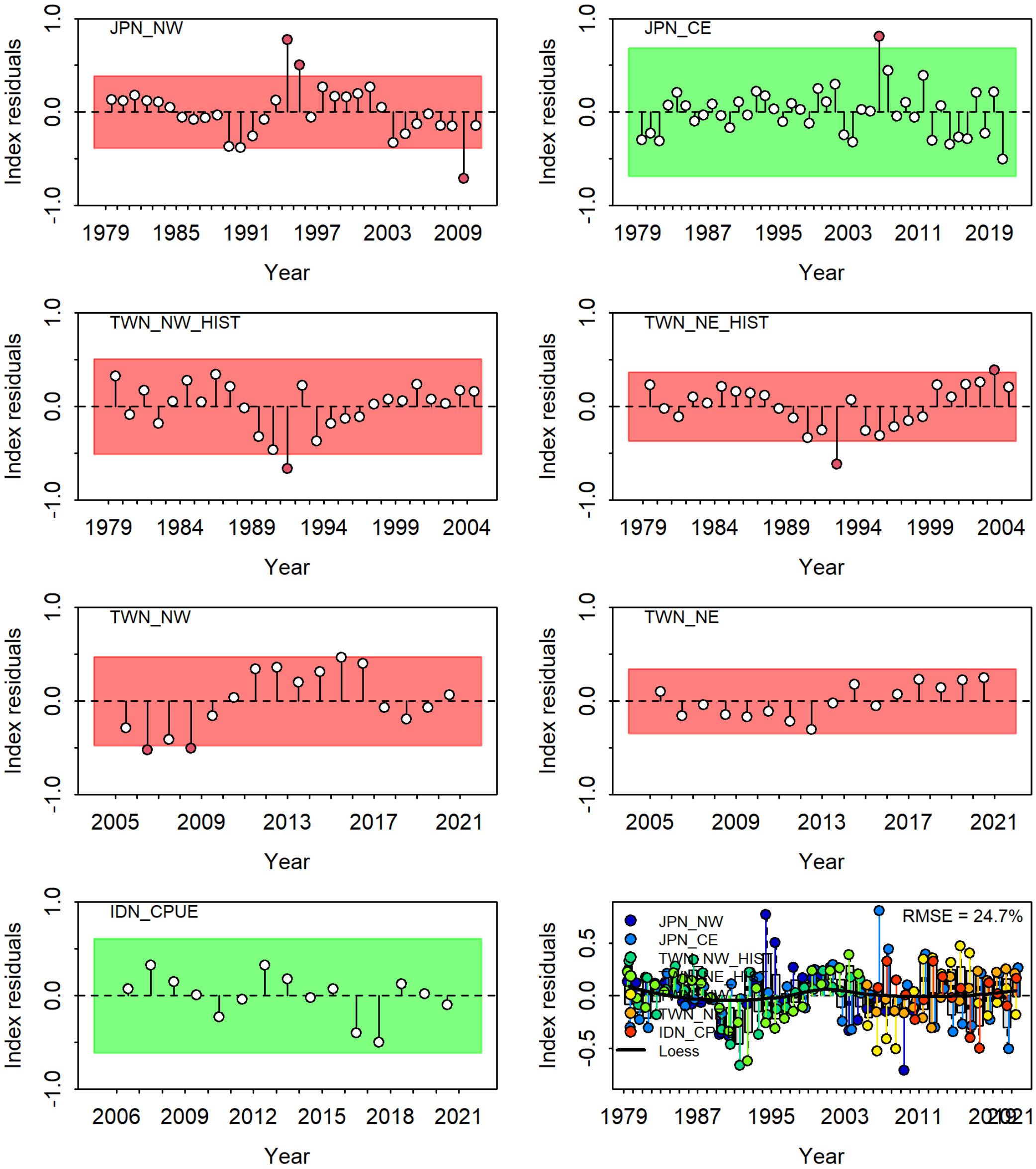

Fig. 9. (continued).

Scenario "S3"

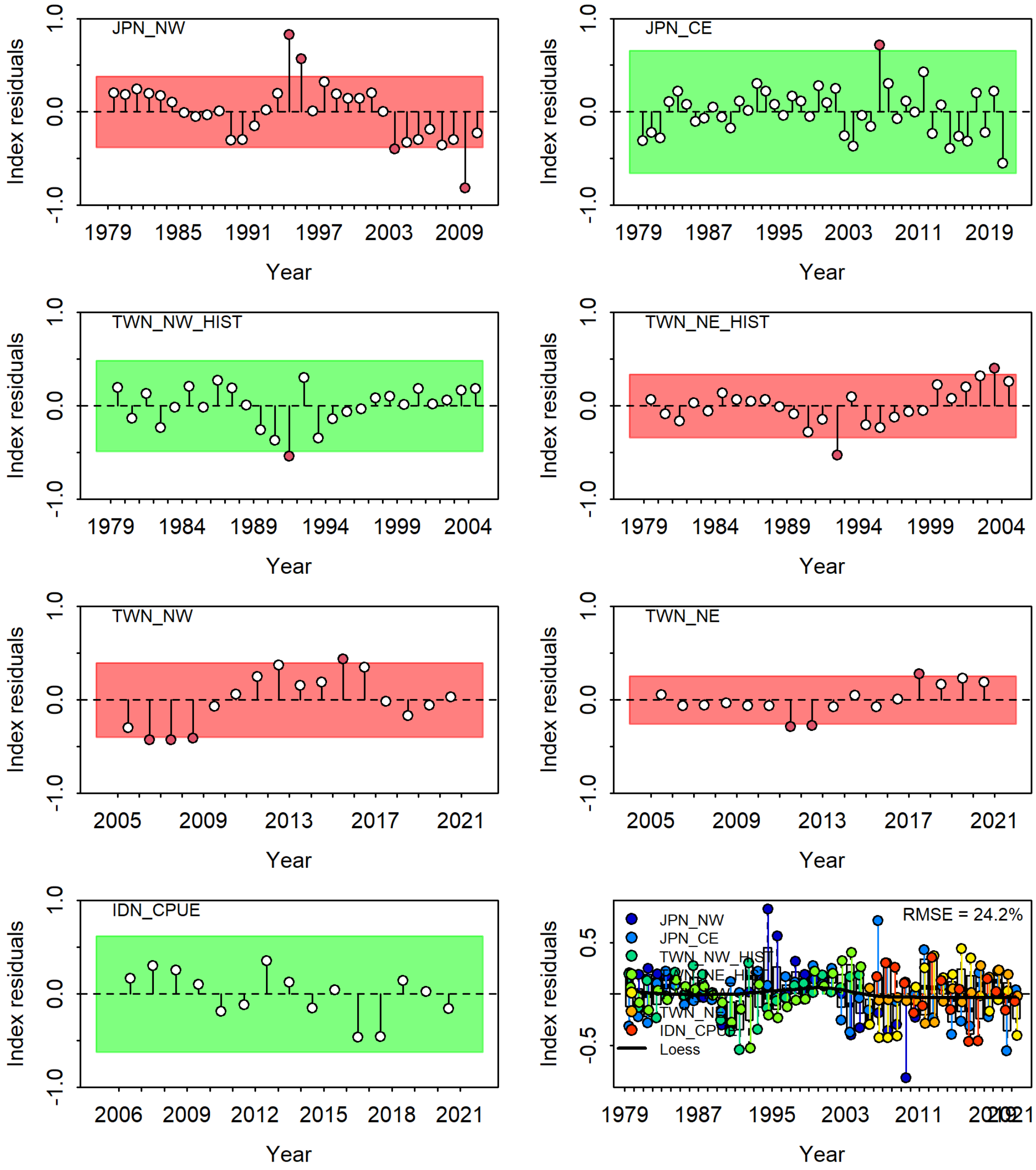

Fig. 9. (continued).

Scenario “S4”

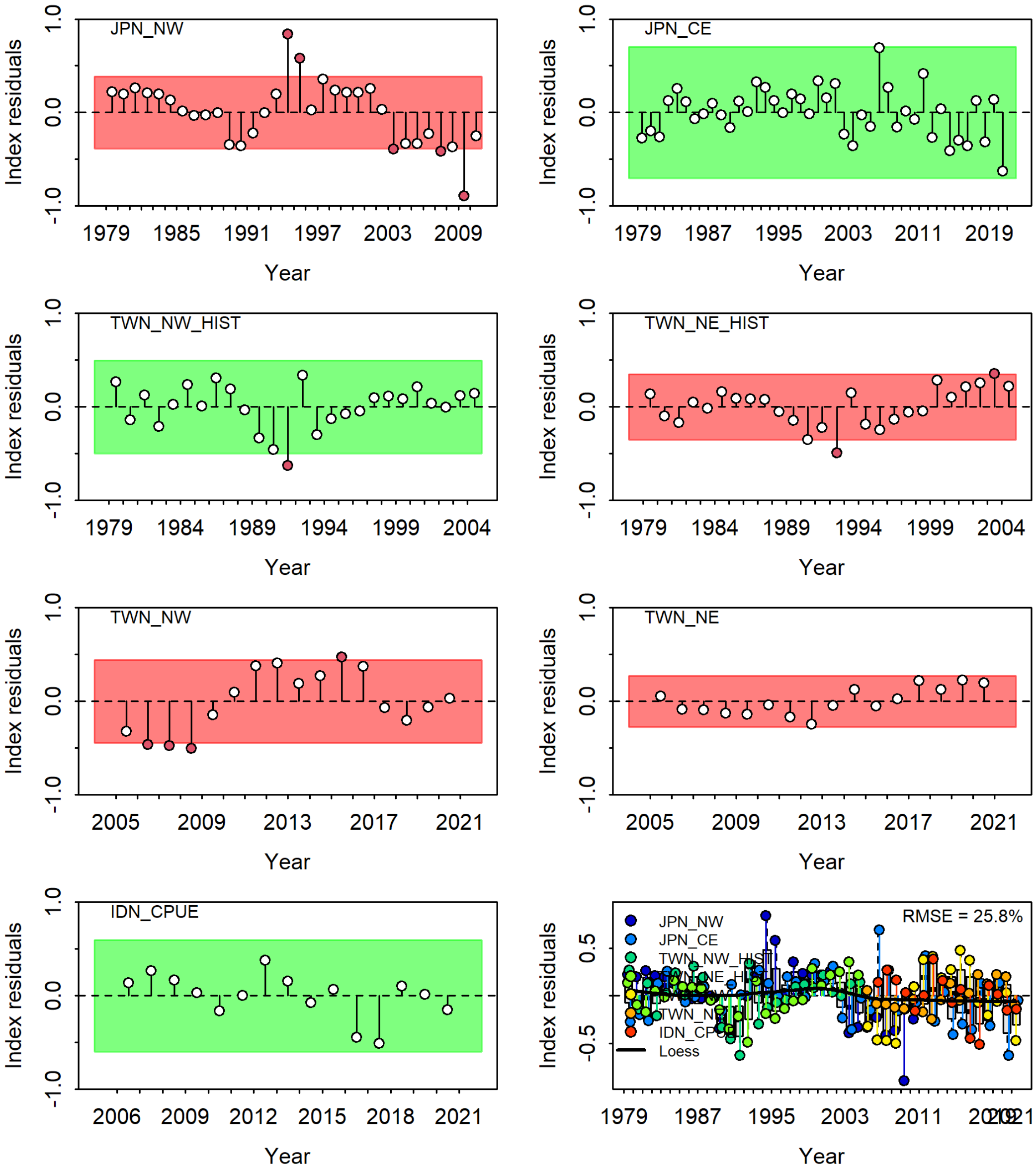

Fig. 9. (continued).

Scenario "S5"

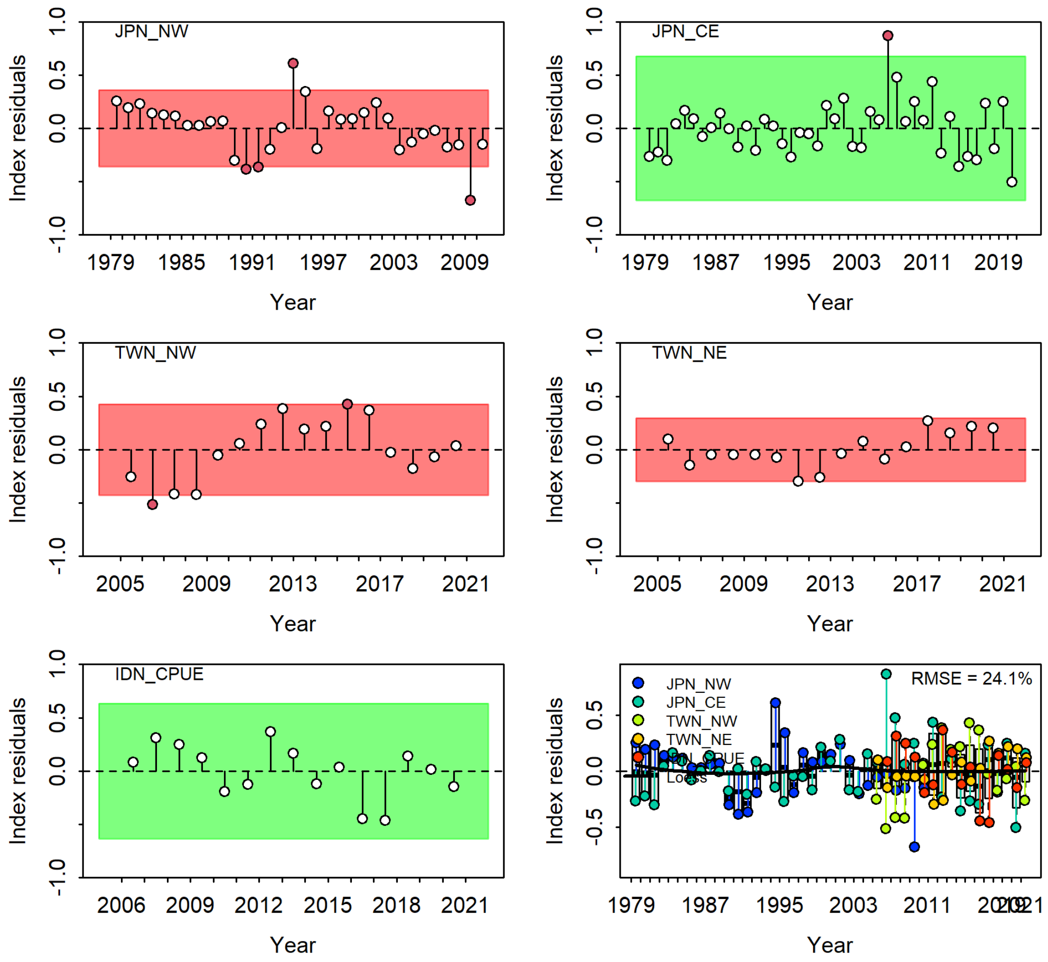

Fig. 9. (continued).

Scenario “S6”

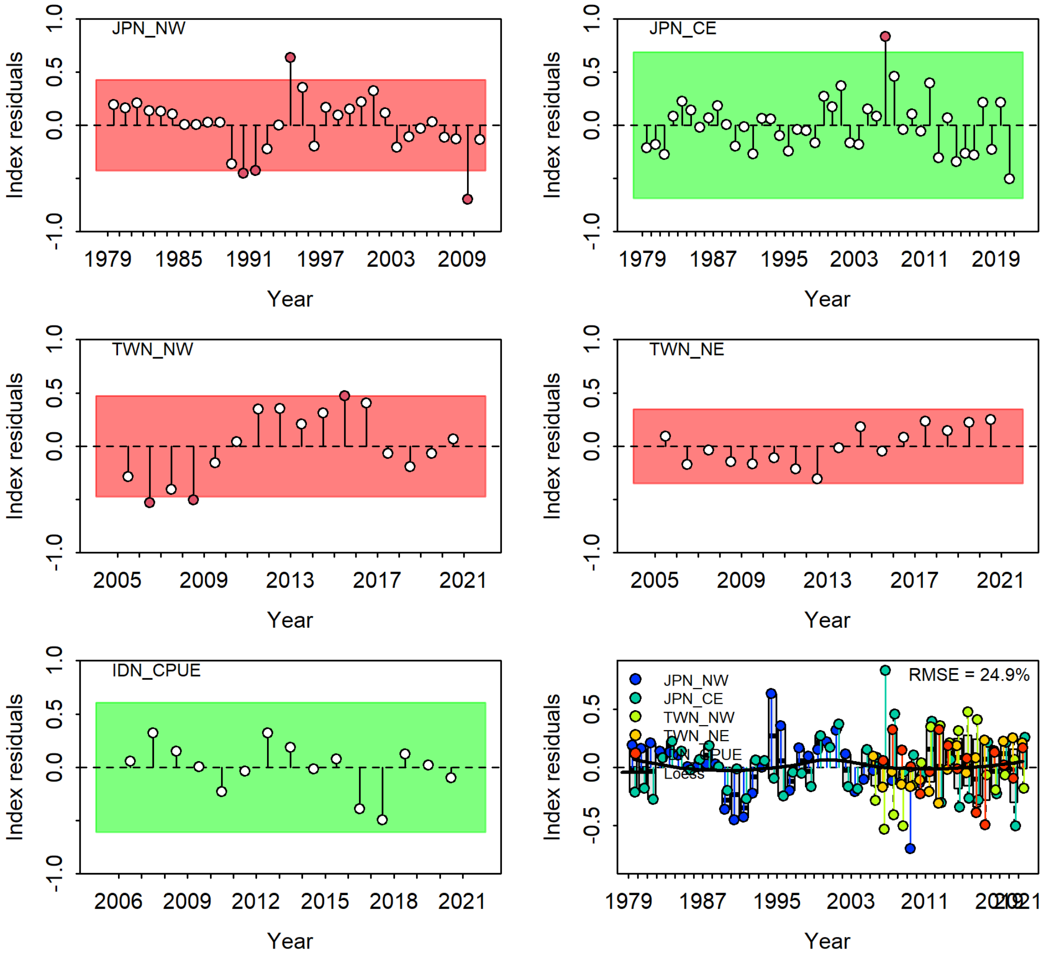

Fig. 9. (continued).

Scenario “S7”

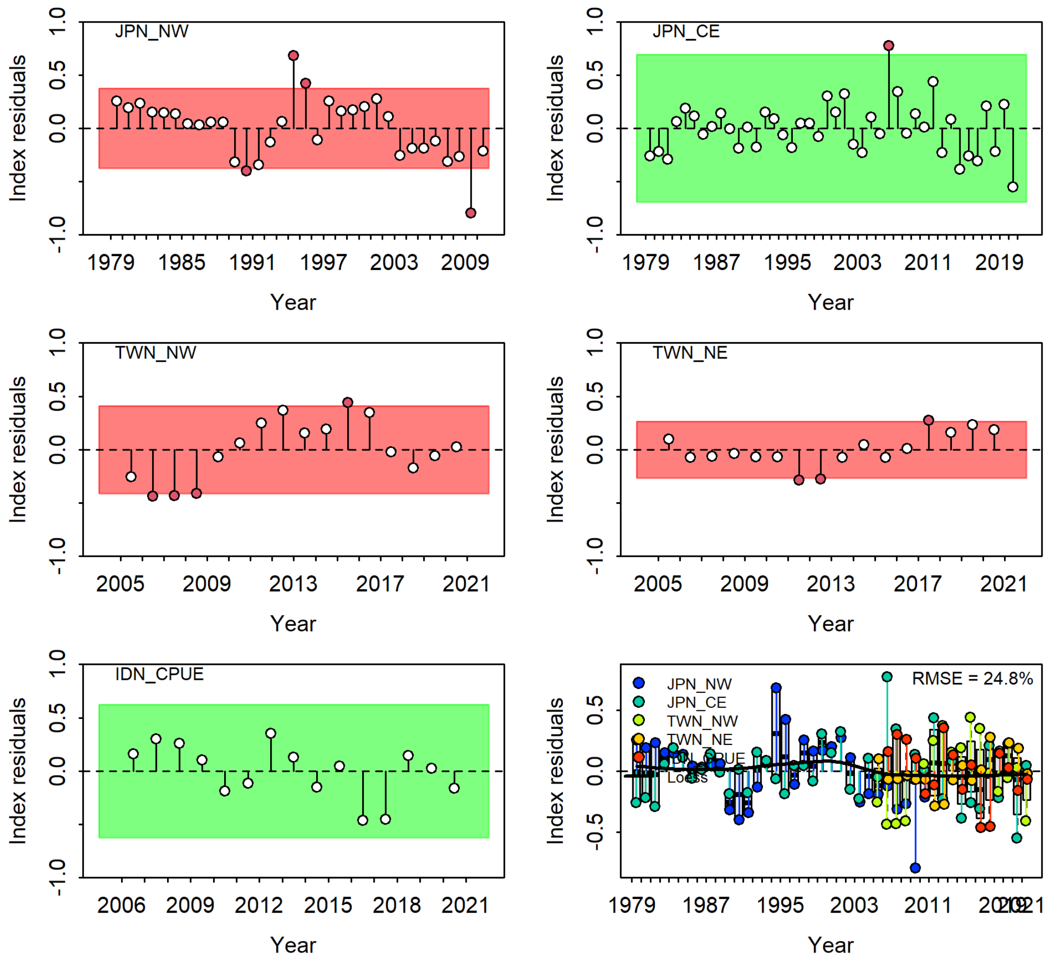

Fig. 9. (continued).

Scenario "S8"

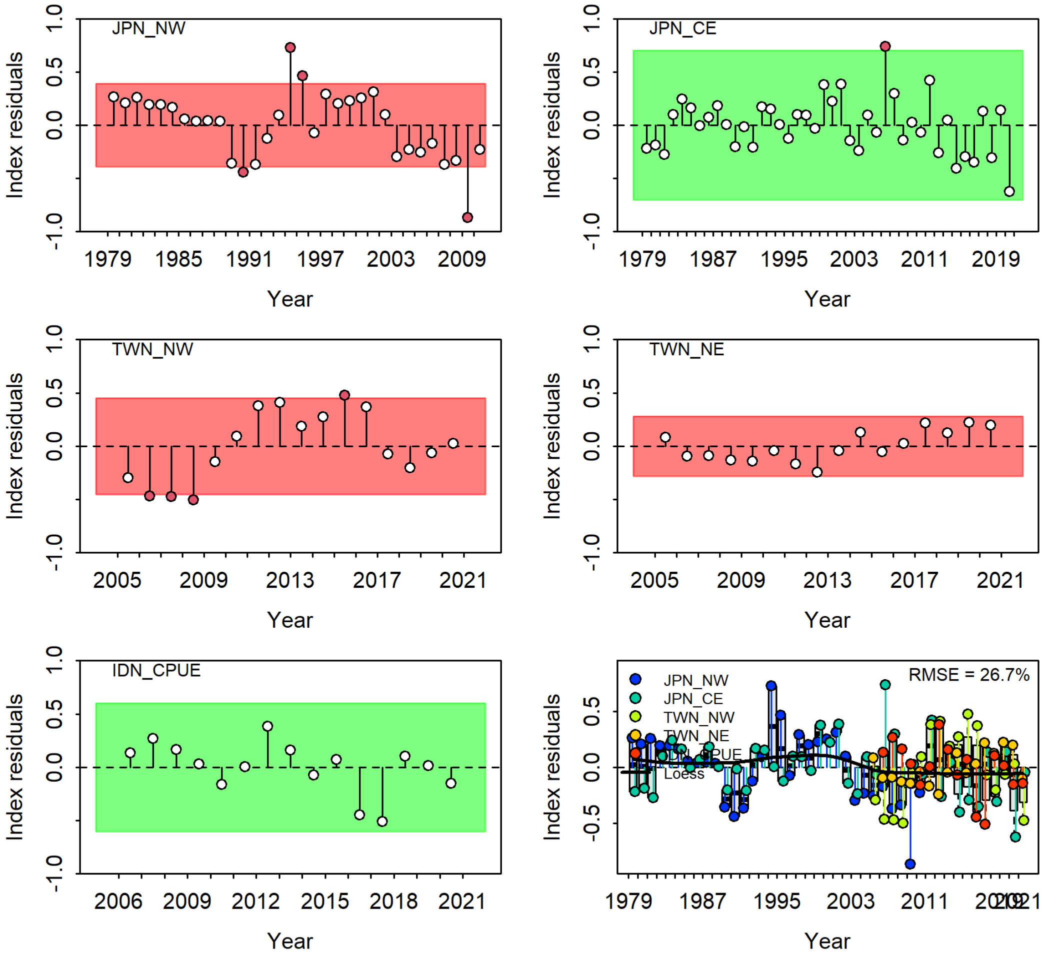

Fig. 9. (continued).

Scenario "S9"

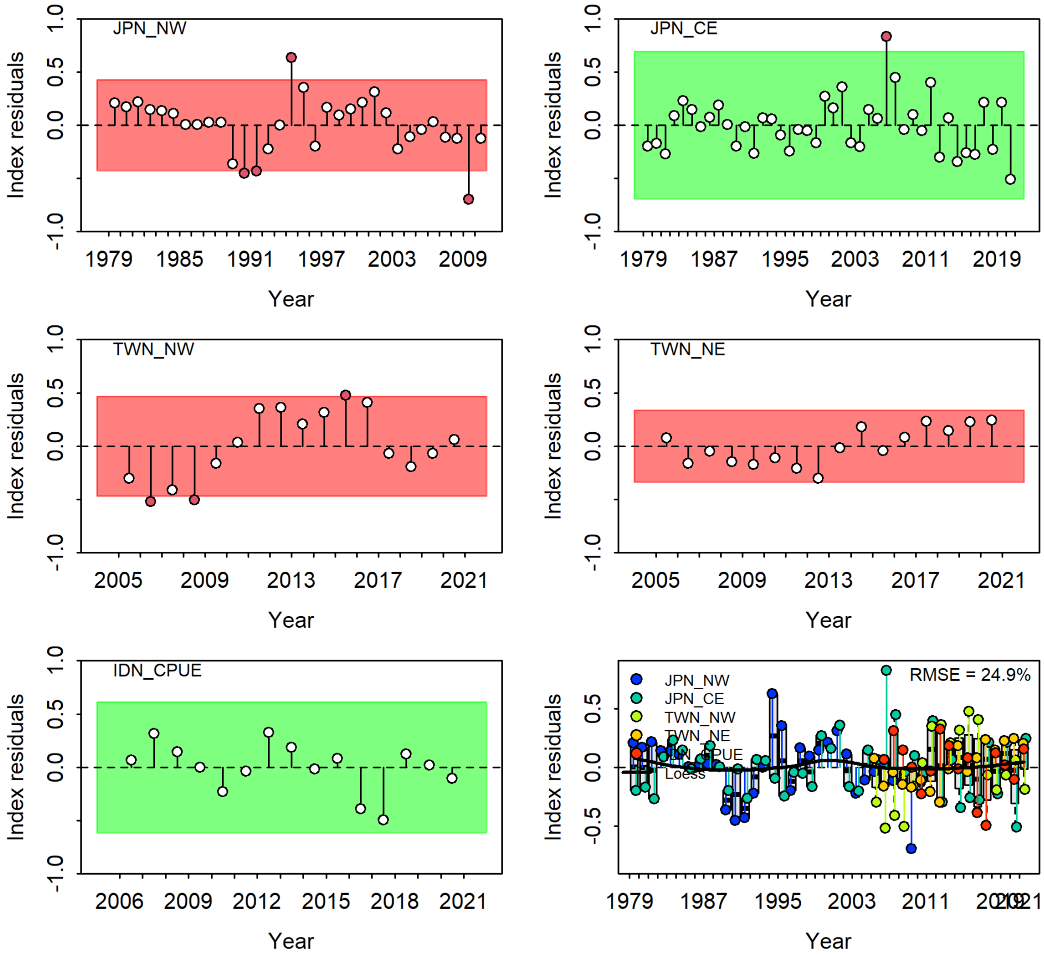

Fig. 9. (continued).

Scenario "S10"

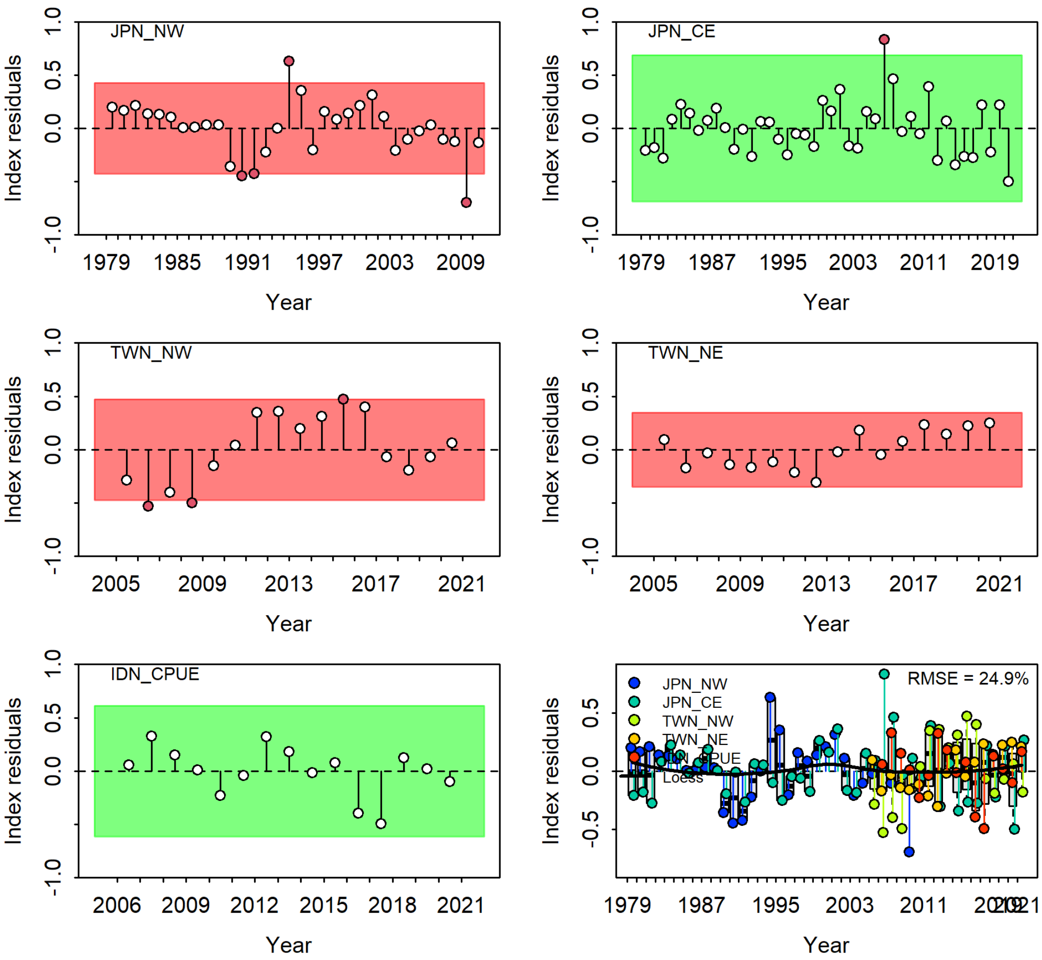

Fig. 9. (continued).

Scenario "S1"

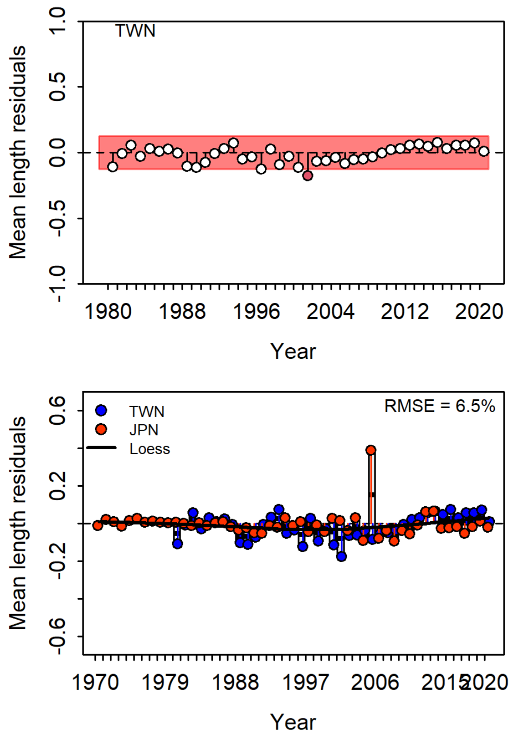

Fig. 10. Runs test plot (green shading indicates no evidence ($p \geq 0.05$) and red shading evidence ($p < 0.05$) to reject the hypothesis of a randomly distributed time-series of residuals, respectively) and joint residual plot for fits to length-frequency data (vertical lines with points show the residuals, and solid black lines show loess smoother through all residuals, boxplots indicate the median and quantiles in cases where residuals from the multiple indices are available for any given year and root mean squared errors (RMSE) are included in the upper right-hand corner of each plot).

Scenario "S2"

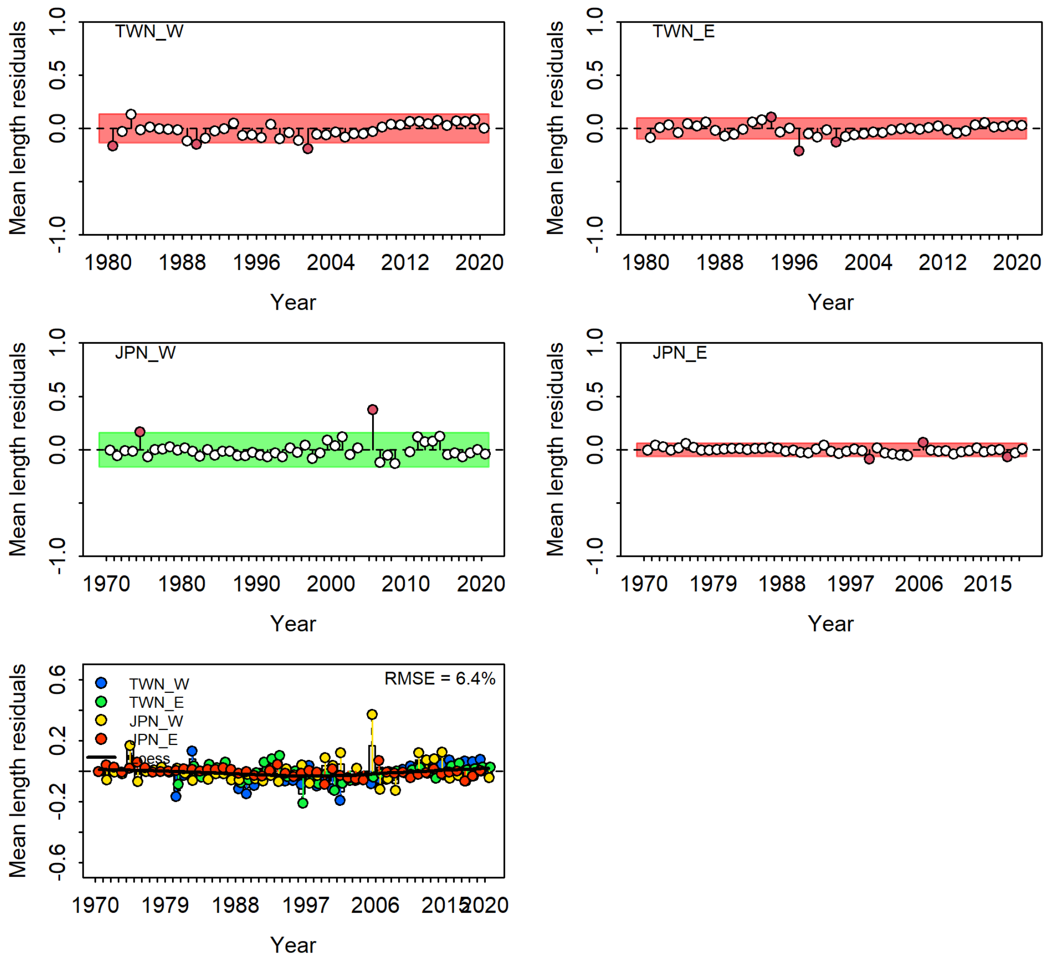

Fig. 10. (continued).

Scenario “S3”

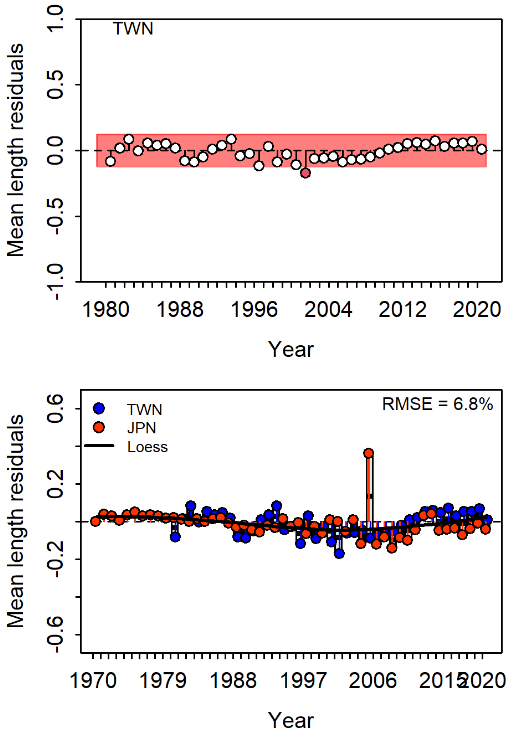

Fig. 10. (continued).

Scenario “S4”

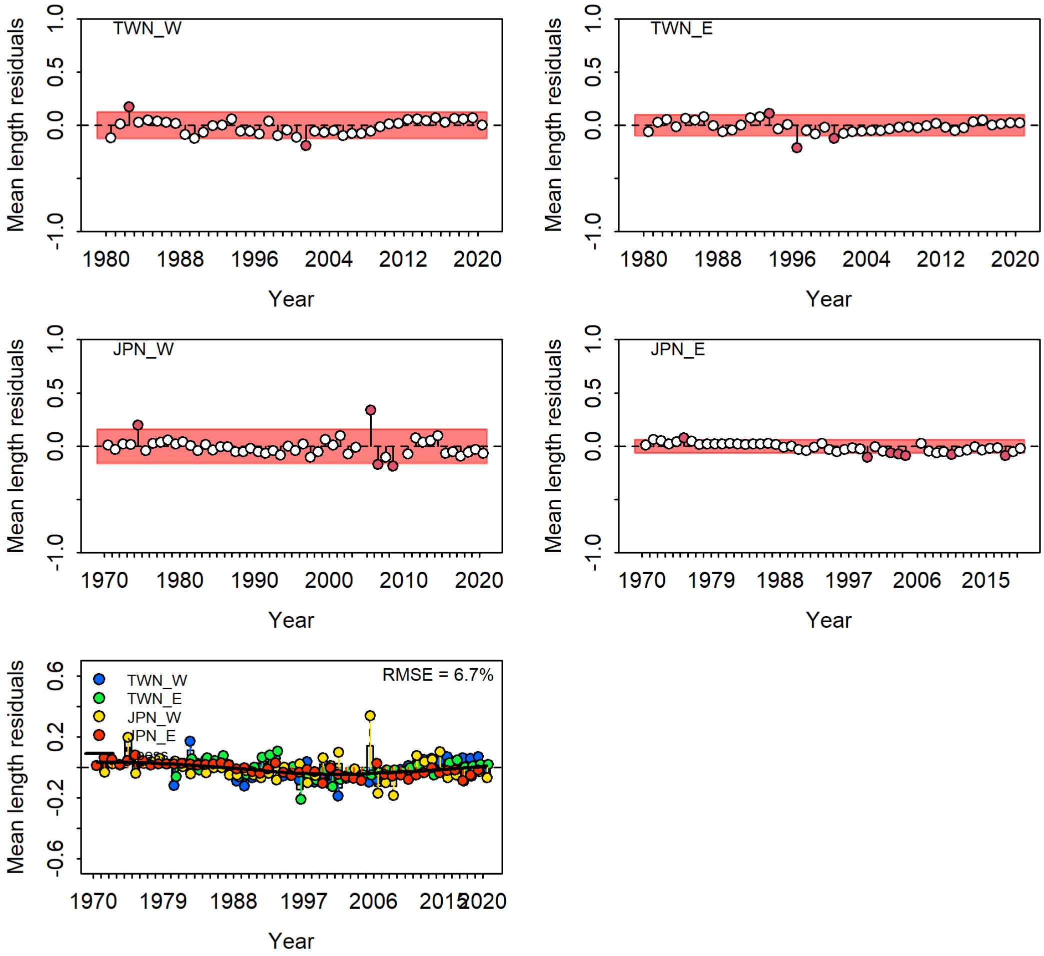

Fig. 10. (continued).

Scenario “S5”

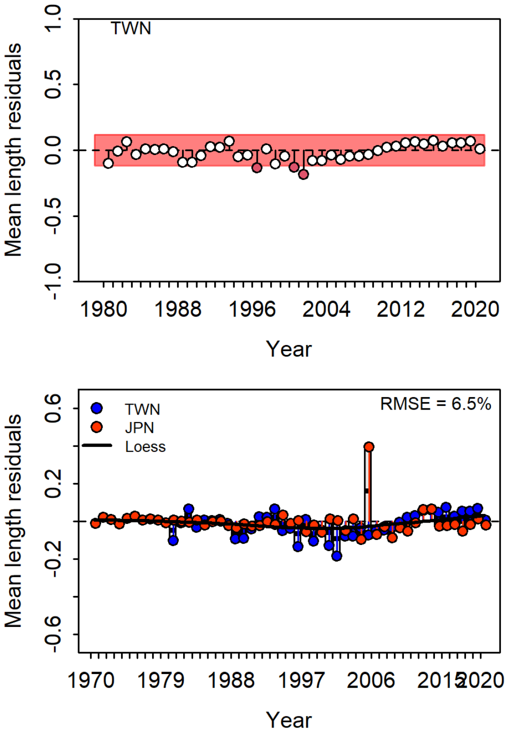

Fig. 10. (continued).

Scenario "S6"

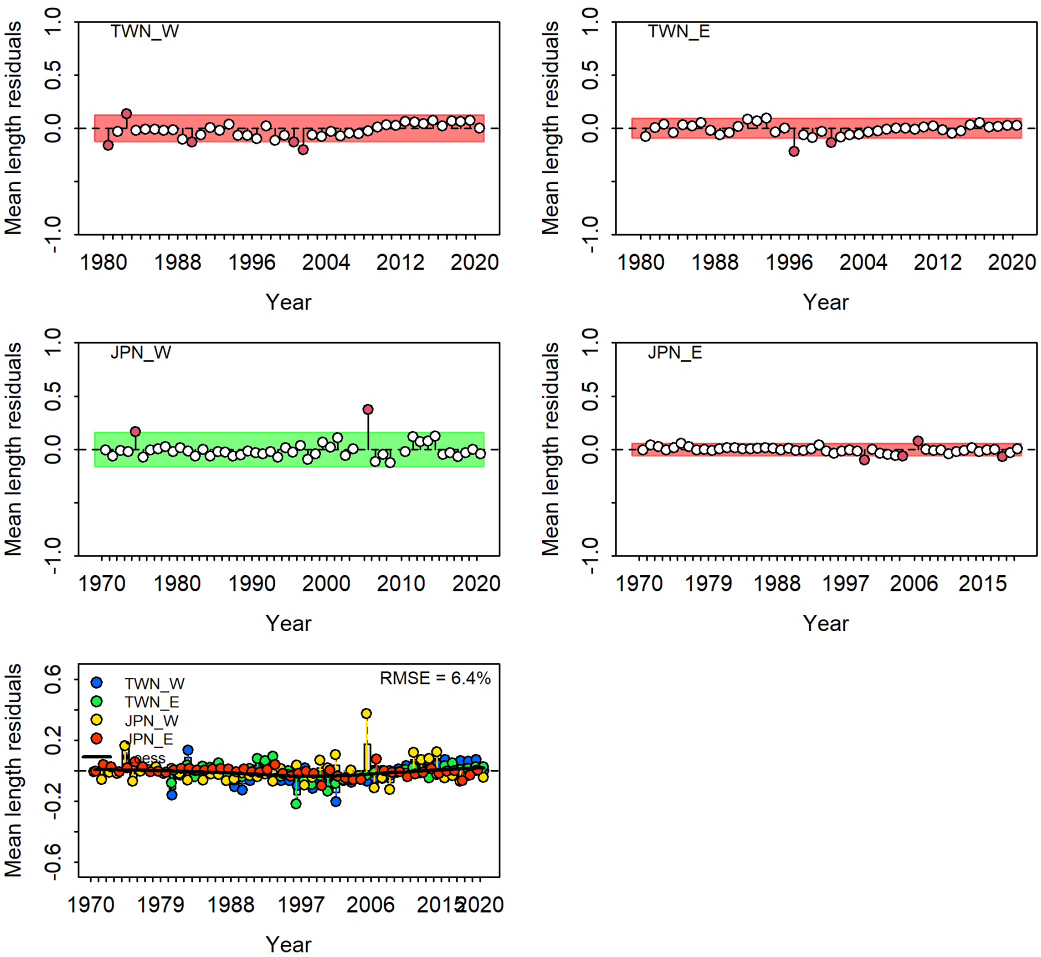

Fig. 10. (continued).

Scenario "S7"

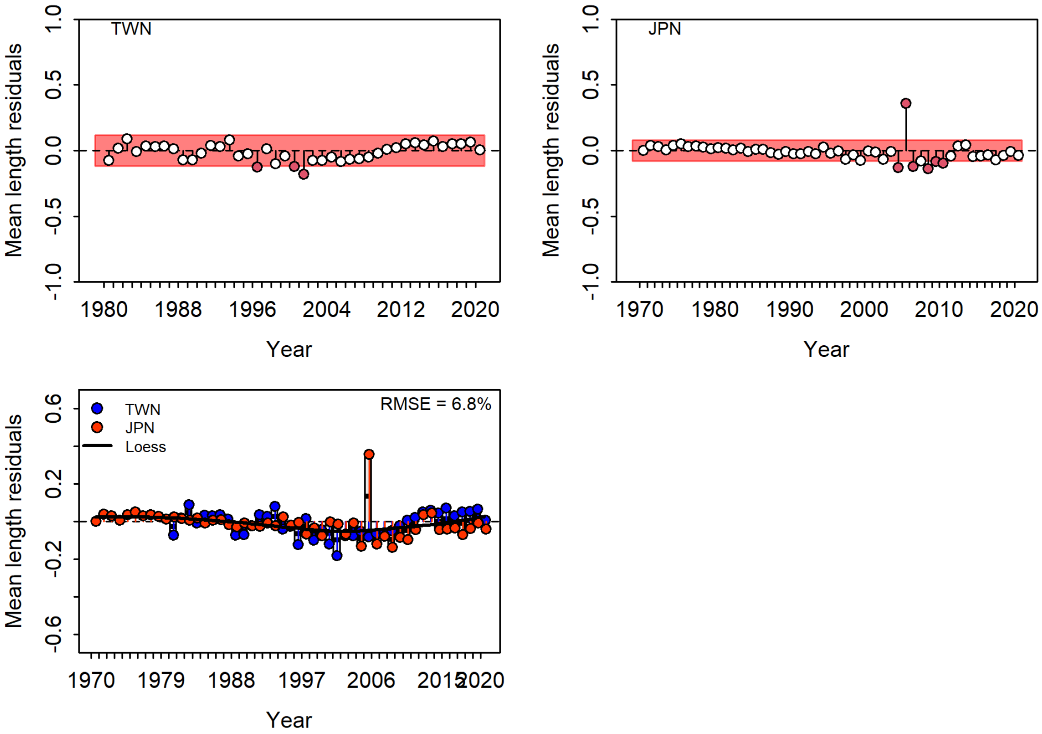

Fig. 10. (continued).

Scenario “S8”

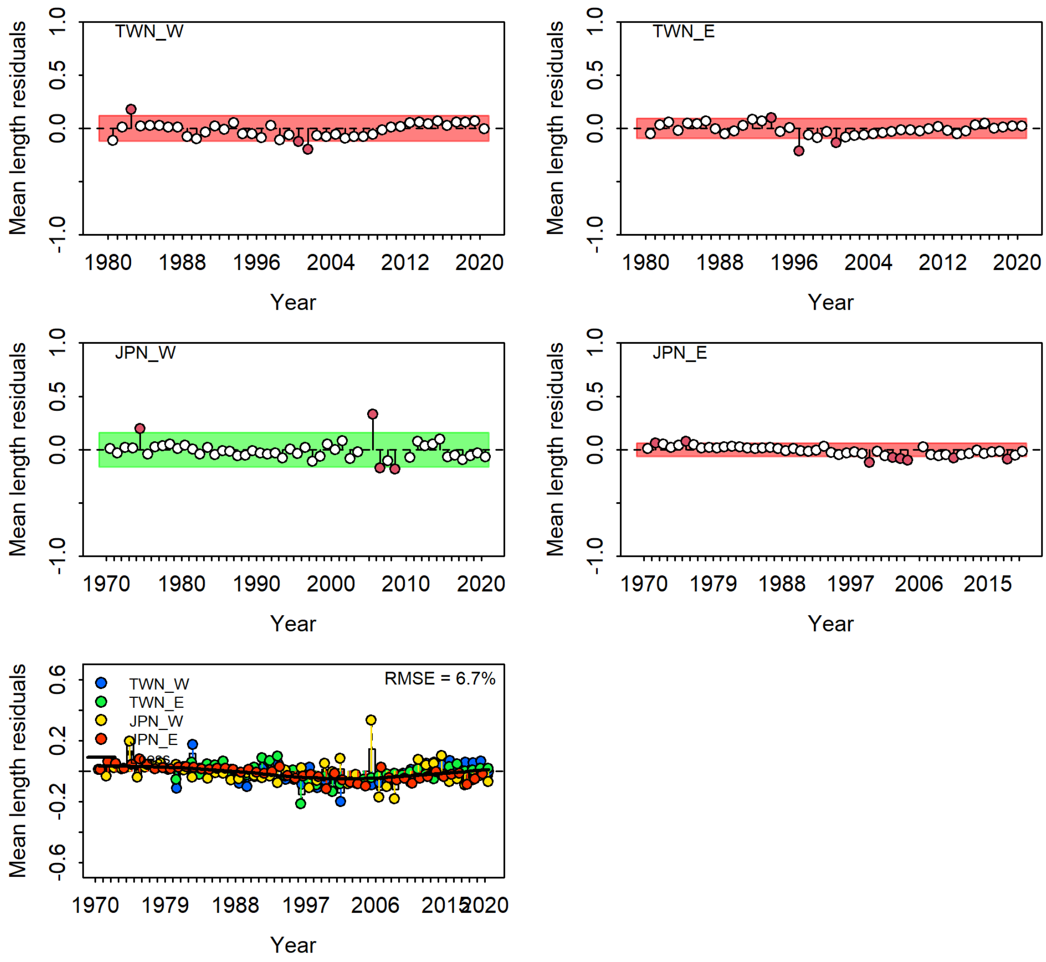

Fig. 10. (continued).

Scenario "S9"

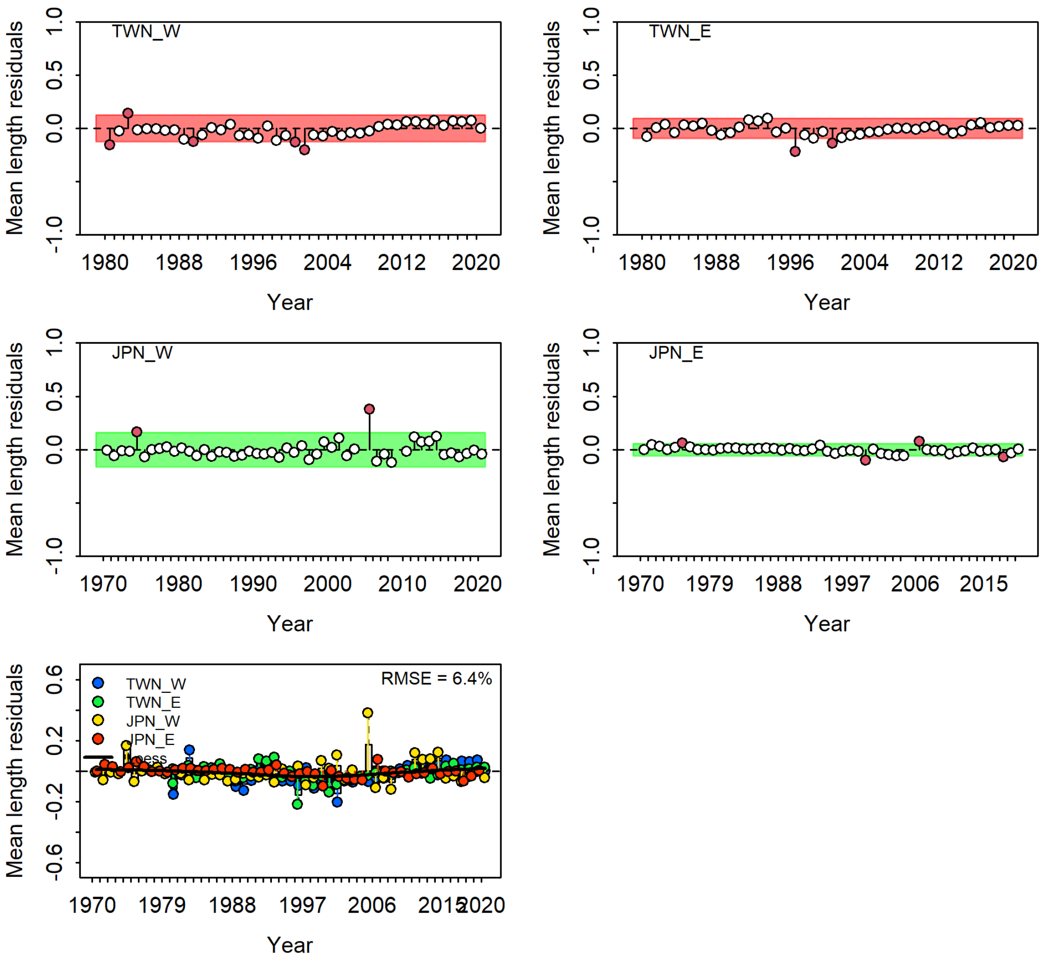

Fig. 10. (continued).

Scenario "S10"

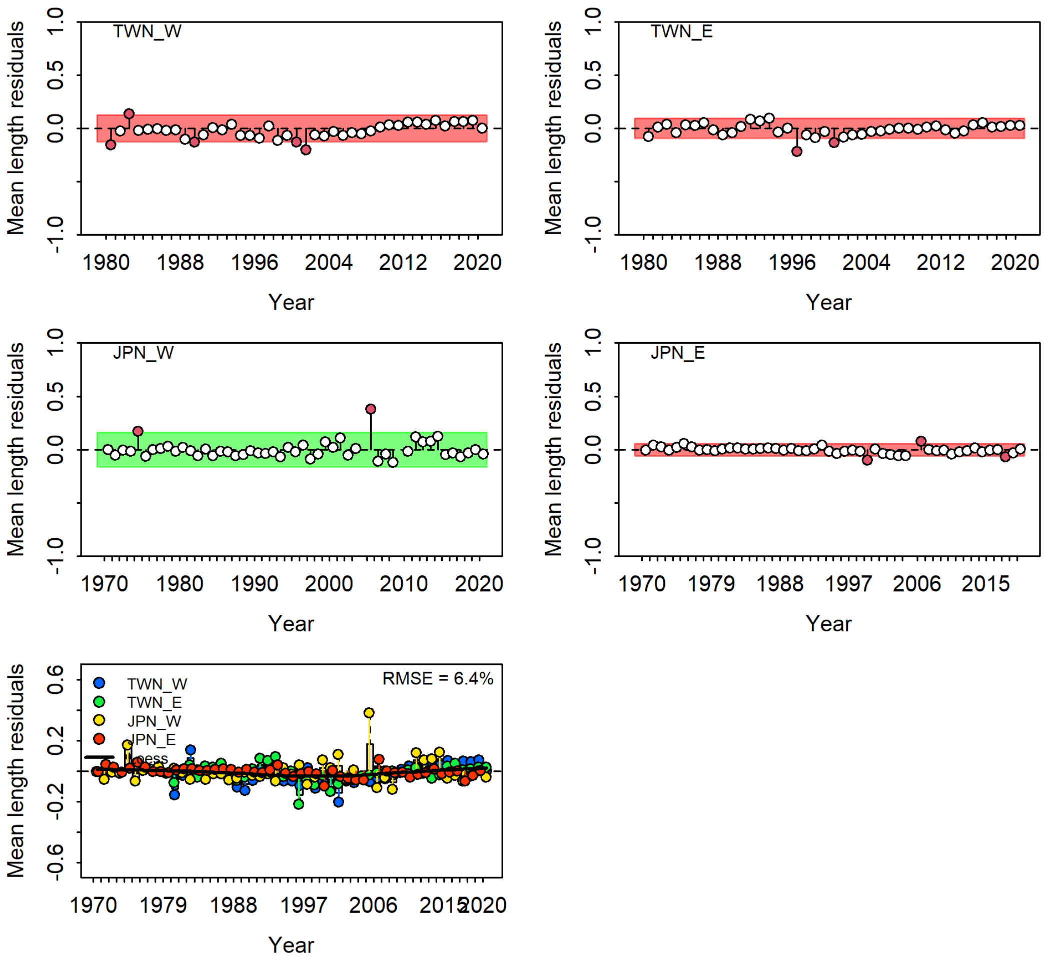

Fig. 10. (continued).

One-area scenarios

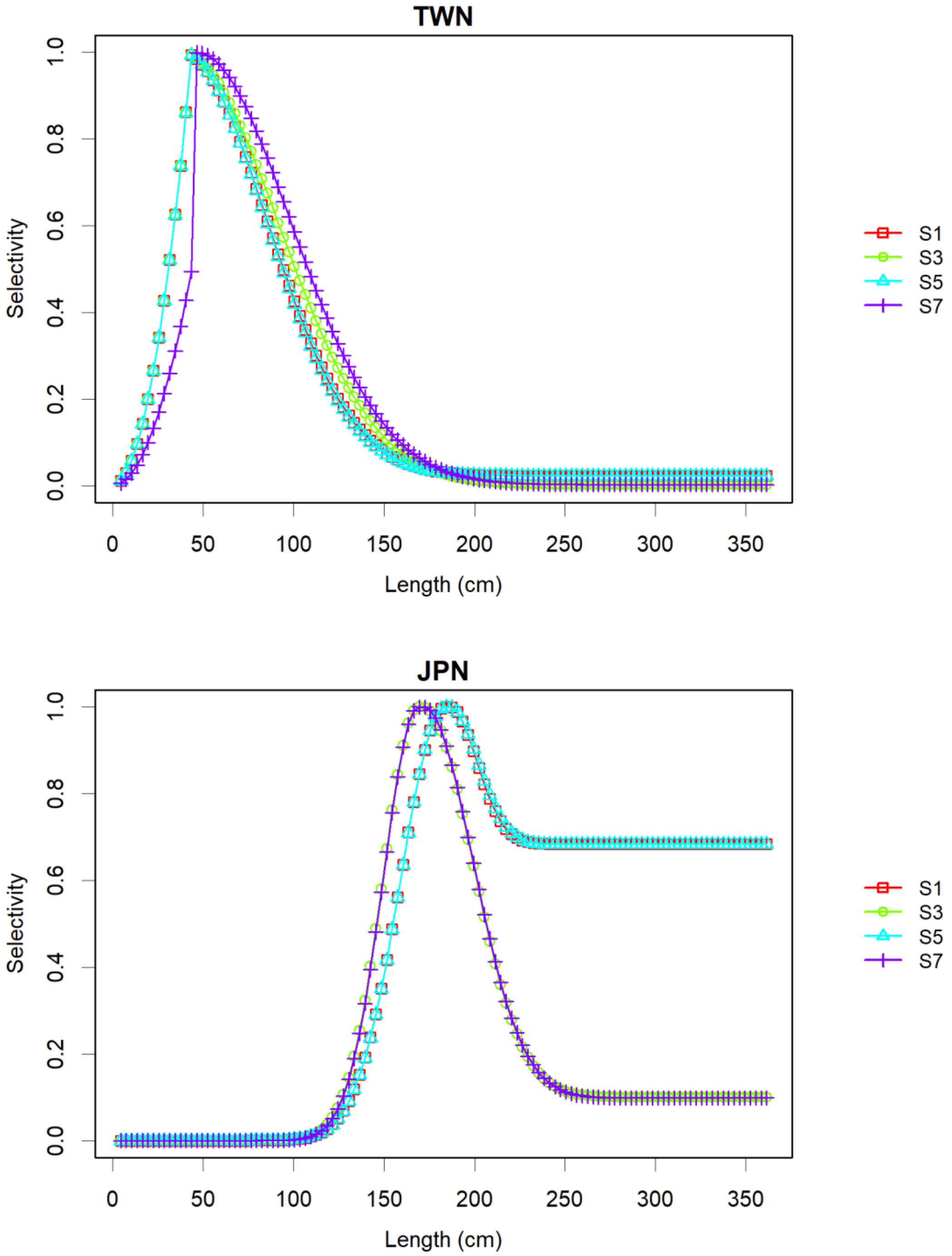

Fig. 11. Model-estimated selectivity for blue marlin in the Indian Ocean.

Two-area scenarios

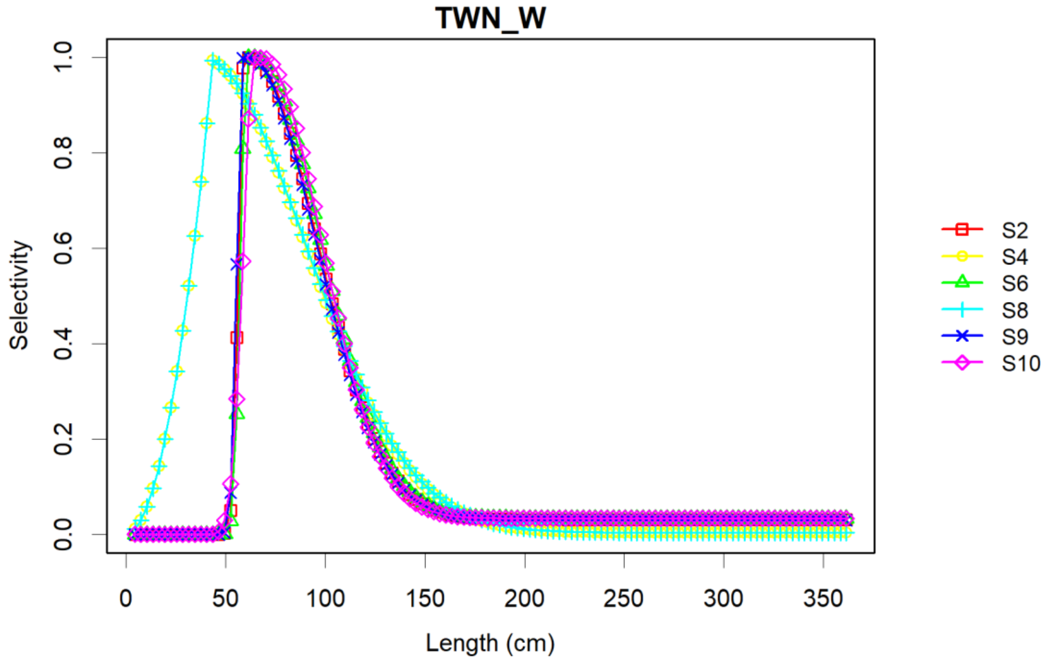

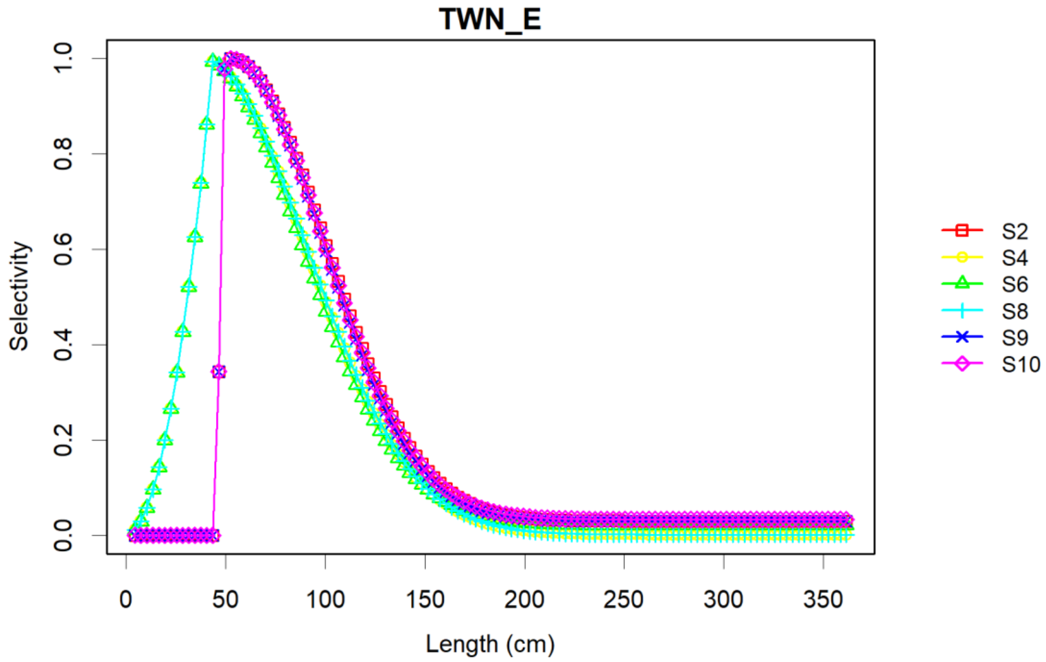

Fig. 11. (continued).

Two-area scenarios

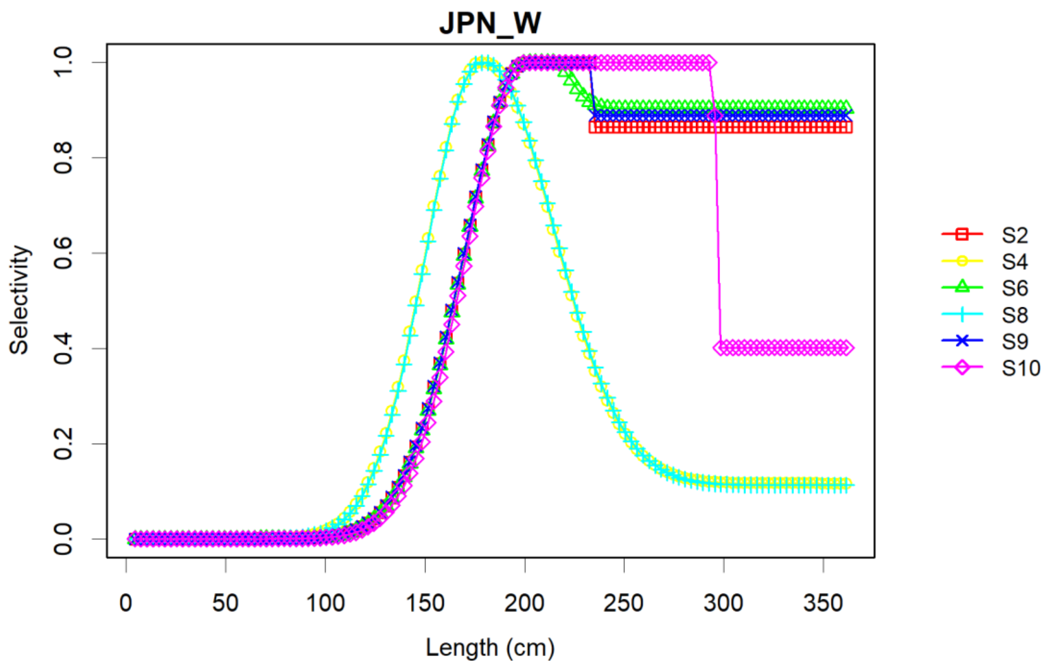

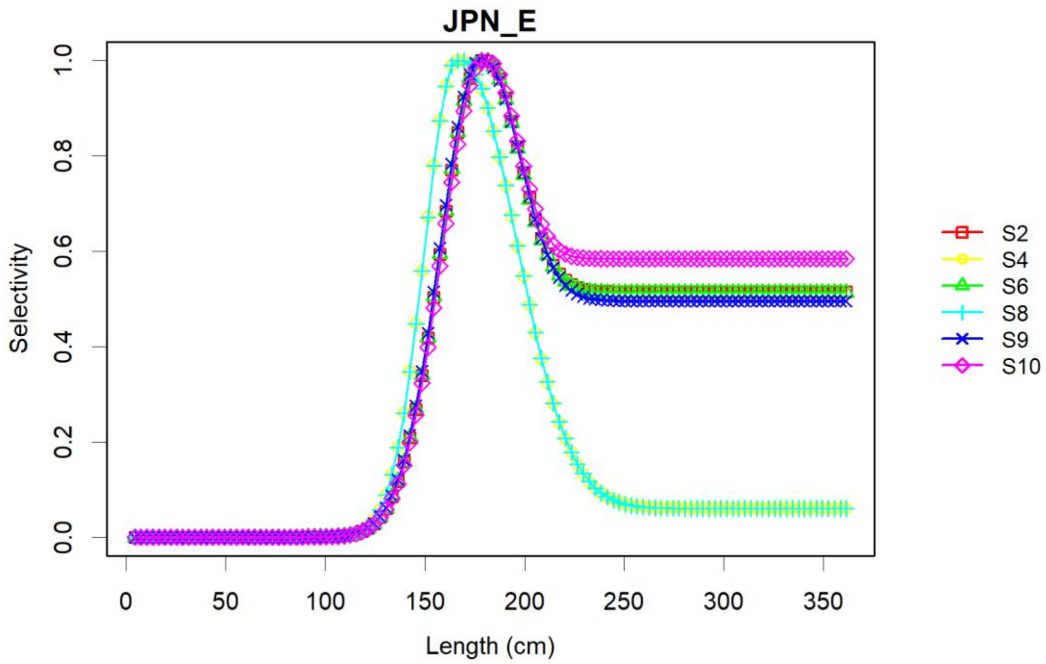

Fig. 11. (continued).

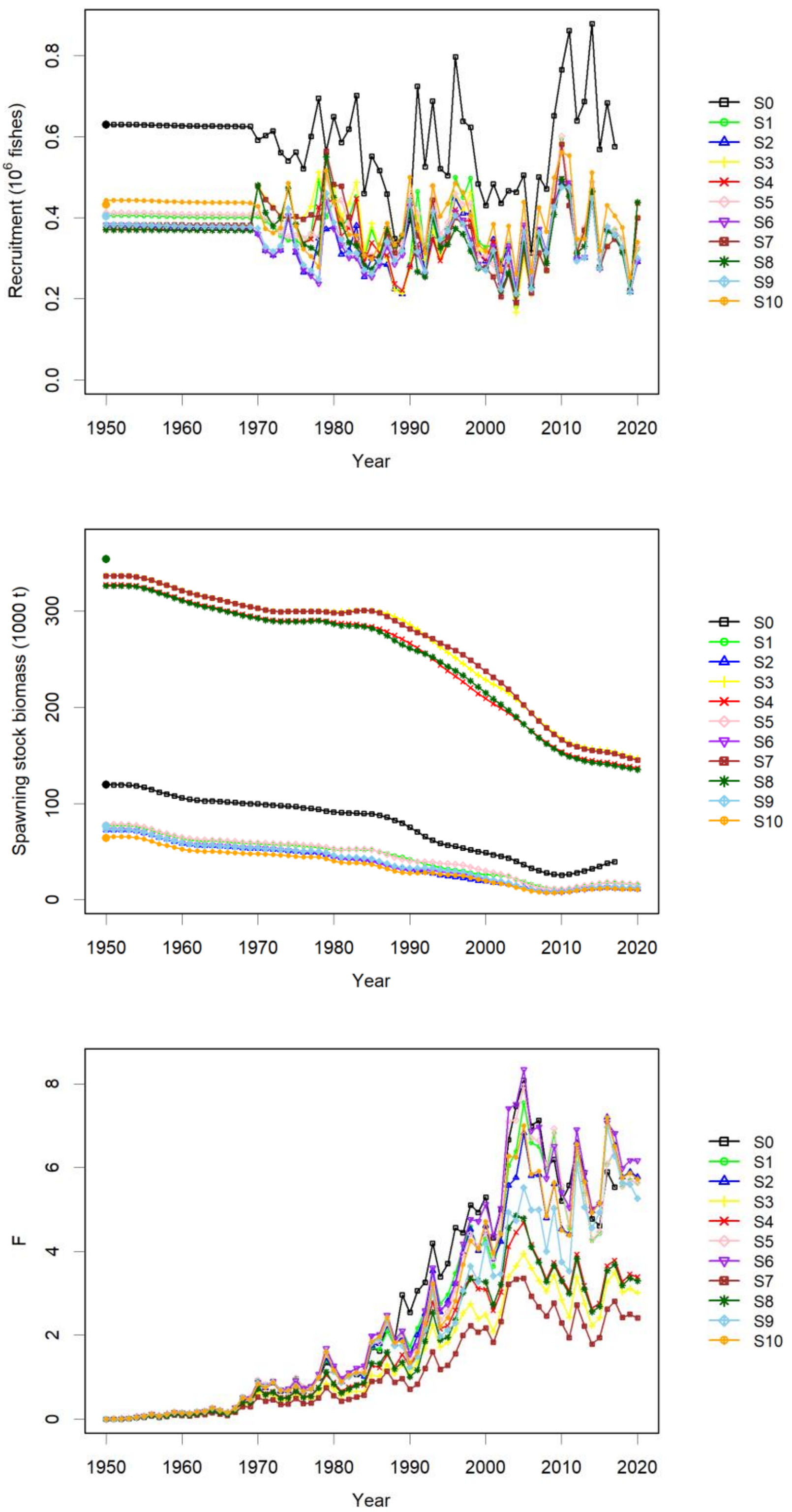

Fig. 12. Time trajectories of the model-estimated recruitment, spawning biomass and fishing mortality of blue marlin in the Indian Ocean.

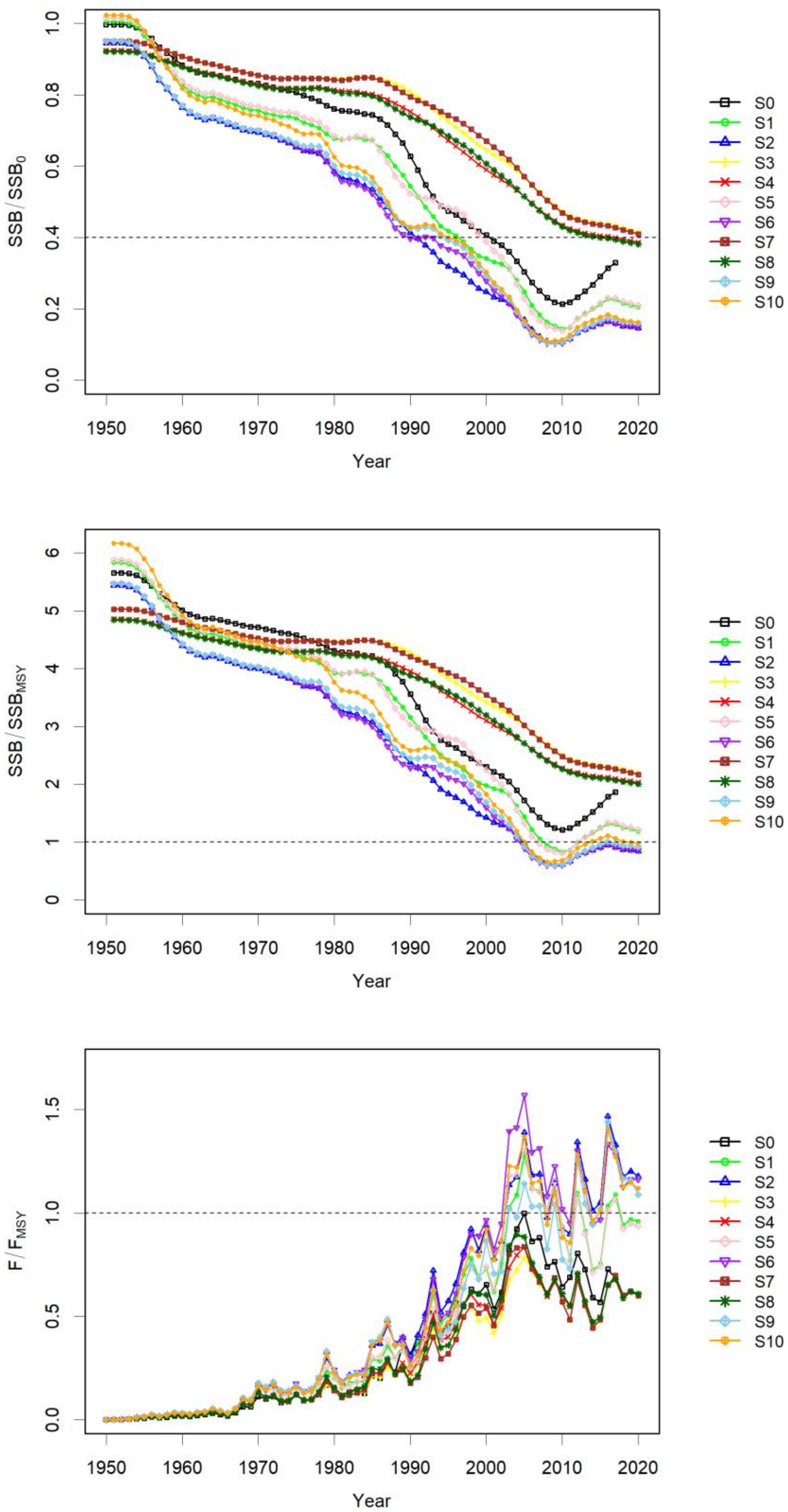

Fig. 13. Time trajectory of the model-estimated relative fishing mortality and spawning biomass of blue marlin in the Indian Ocean.

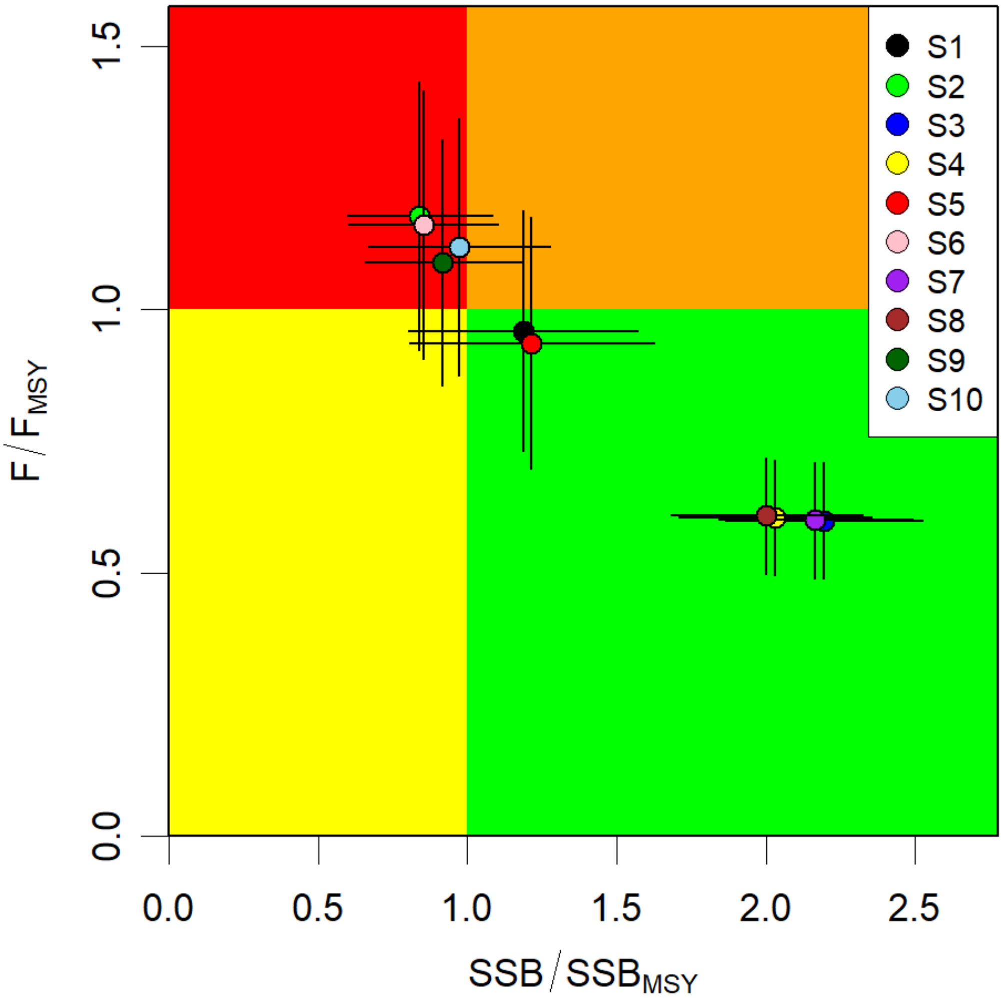

Fig. 14. Kobe plot for blue marlin in the Indian Ocean.

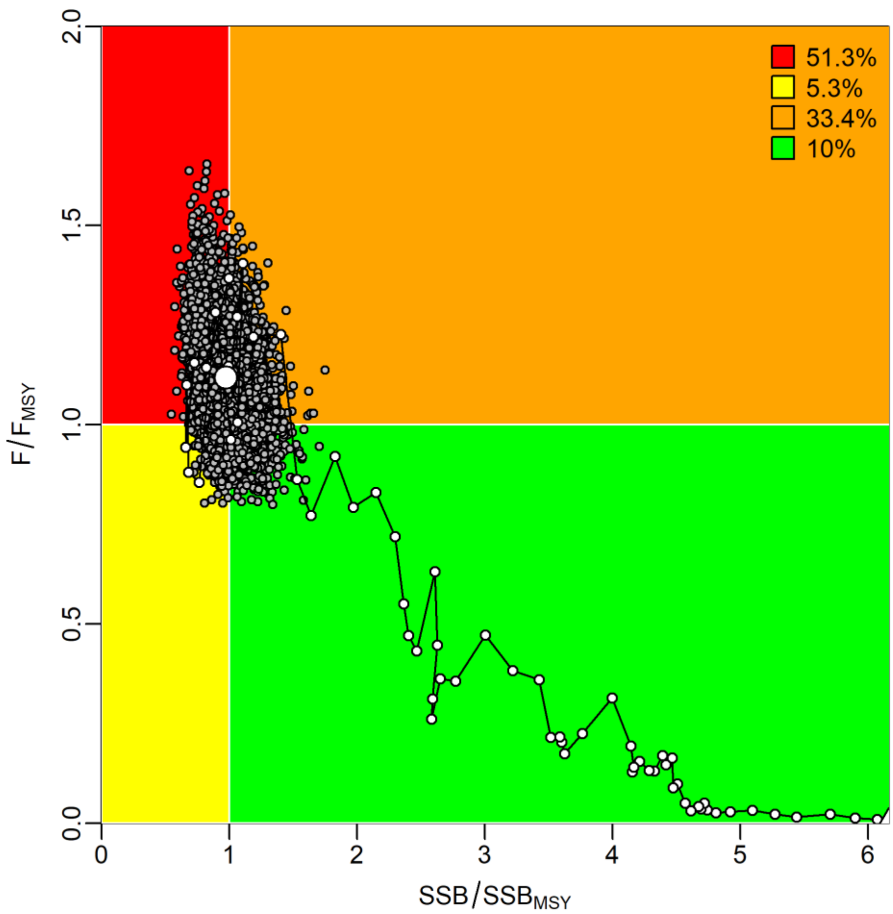

Fig. 15. Kobe plot for blue marlin in the Indian Ocean obtained from selected scenario (S10).

Table 1. Life-history parameters of blue marlin used in this study.

Parameter	Female	Male
Natural mortality (*M*, year^{-1})	0.22	0.37
Length at youngest age (*L*1, cm)	144.000	144.000
Length at oldest age (*L*2, cm)	304.178	226.000
Growth coefficient (*K*, year^{-1})	0.107	0.211
Length-Weight (*a*)	1.844E−05	1.37E−05
Length-Weight (*b*)	2.956	2.975
Length at 50% maturity (cm)	179.76	
Maturity slope	-0.25	
Spawner-recruit steepness (*h*)	0.87	0.87
Variation in recruitment (σ)	0.4	0.4

Table 2. Model assumptions of scenarios conducted for sensitivity analysis.

Scenario	Area	Fleet	CPUE used	Natural Mortality
S0	1	TWN, JPN, IDN and OTH	JPN_NW+JPN_CE+TWN_NW+TWN_NE+IDN (“S7” of the previous assessment in 2019)	Fixed
S1	1	TWN, JPN, IDN and OTH	JPN_NW+JPN_CE+TWN_NW_HIST (1979-2004) +TWN_NE_HIST (1979-2004)+TWN_NW (2005-2020) +TWN_NE (2005-2020)+IDN	Fixed
S2	2 (E+W)	TWN_W, TWN_W, JPN_W, JPN_E, IDN, OTH_W and OTH_E	Same with “S1”	Fixed
S3	1	TWN, JPN, IDN and OTH	Same with “S1”	Age-specific
S4	2 (E+W)	TWN_W, TWN_W, JPN_W, JPN_E, IDN, OTH_W and OTH_E	Same with “S1”	Age-specific
S5	1	TWN, JPN, IDN and OTH	Same with “S1” but TWN_NW_HIST (1979-2004) and TWN_NE_HIST (1979-2004) were excluded	Fixed
S6	2 (E+W)	TWN_W, TWN_W, JPN_W, JPN_E, IDN, OTH_W and OTH_E	Same with “S5”	Fixed
S7	1	TWN, JPN, IDN and OTH	Same with “S5”	Age-specific
S8	2 (E+W)	TWN_W, TWN_W, JPN_W, JPN_E, IDN, OTH_W and OTH_E	Same with “S5”	Age-specific
S9	Same with “S6” but selectivity of IDN assumed to be the same with JPN_E			
S10	Same with “S8” but the mean values of age-specific natural mortalities were scaled to the same as fixed natural mortality			

Table 3. The estimates of key management quantities for blue marlin in the Indian Ocean.

Scenario	R_0	SSB_0	MSY	F_{MSY}	SSB_{MSY}	SSB_{2020}/SSB_0	SSB_{2020}/SSB_{MSY}	F_{2020}/F_{MSY}
S0	405,784	119,723	11,217	8.103	21,120	0.333	1.885	0.772
S1	381,638	76,650	8,079	5.881	13,224	0.205	1.187	0.960
S2	383,914	76,650	8,123	4.910	13,332	0.146	0.841	1.177
S3	373,018	354,280	10,266	5.028	67,008	0.415	2.195	0.599
S4	411,724	354,280	10,251	5.599	67,464	0.387	2.030	0.606
S5	383,415	77,021	8,129	6.019	13,307	0.210	1.216	0.937
S6	383,729	76,650	8,131	5.313	13,341	0.148	0.853	1.161
S7	371,809	354,280	10,314	4.027	67,001	0.410	2.167	0.600
S8	383,655	354,280	10,273	5.420	67,453	0.381	2.003	0.609
S9	442,876	766,450	8,253	4.837	13,323	0.160	0.920	1.089
S10	405,784	64,053	7,572	5.118	10,641	0.162	0.974	1.119

Table 4. Stock status summary table for the blue marlin SS3 assessment (model S10).

Management Quantity (model S10)	**Aggregate Indian Ocean**
2020 catch estimate	7,126 (t)
Mean catch from 2016–2020	8,753 (t)
MSY (1000 t) (80% CI)	7.572 (6.496, 8.648)
Data period (catch)	1950–2020
F_{MSY} (80% CI)*	5.118 (4.545, 5.691)
SB_{MSY} (1,000 t) (80% CI)	10.641 (9.116, 12.167)
F_{2020}/F_{MSY} (80% CI)	1.119 (0.959, 1.279)
SB_{2020}/SB_{MSY} (80% CI)	0.974 (0.774, 1.173)
SB_{2020}/SB_{1950} (80% CI)	0.158 (0.134, 0.180)

Table 5. Kobe II Strategy Matrix for blue marlin in the Indian Ocean obtained from selected scenario (S10). Probability (percentage) of exceeding the MSY-based target reference points under the constant catch with 10-110% of the 2020 catch level (7,126 t) for 10 years projection.

Pr (SSB < SSB_{MSY})										
Catch	2021	2022	2023	2024	2025	2026	2027	2028	2029	2030
10%	0.66	0.23	0.01	0.00	0.00	0.00	0.00	0.00	0.00	0.00
20%	0.66	0.27	0.04	0.00	0.00	0.00	0.00	0.00	0.00	0.00
30%	0.66	0.32	0.07	0.01	0.00	0.00	0.00	0.00	0.00	0.00
40%	0.66	0.38	0.12	0.03	0.00	0.00	0.00	0.00	0.00	0.00
50%	0.66	0.44	0.20	0.06	0.01	0.00	0.00	0.00	0.00	0.00
60%	0.66	0.50	0.29	0.14	0.06	0.02	0.00	0.00	0.00	0.00
70%	0.66	0.56	0.38	0.24	0.14	0.08	0.04	0.02	0.01	0.00
80%	0.66	0.61	0.49	0.38	0.27	0.20	0.14	0.10	0.07	0.05
90%	0.66	0.66	0.60	0.51	0.44	0.38	0.33	0.28	0.25	0.21
100%	0.66	0.72	0.68	0.64	0.60	0.57	0.54	0.53	0.50	0.48
110%	0.66	0.77	0.78	0.75	0.74	0.73	0.73	0.73	0.71	0.71

Pr (F > F_{MSY})										
Catch	2021	2022	2023	2024	2025	2026	2027	2028	2029	2030
10%	0.00	0.00	0.00	0.00	0.00	0.00	0.00	0.00	0.00	0.00
20%	0.00	0.00	0.00	0.00	0.00	0.00	0.00	0.00	0.00	0.00
30%	0.00	0.00	0.00	0.00	0.00	0.00	0.00	0.00	0.00	0.00
40%	0.00	0.00	0.00	0.00	0.00	0.00	0.00	0.00	0.00	0.00
50%	0.00	0.00	0.00	0.00	0.00	0.00	0.00	0.00	0.00	0.00
60%	0.02	0.01	0.00	0.00	0.00	0.00	0.00	0.00	0.00	0.00
70%	0.08	0.04	0.02	0.02	0.01	0.01	0.01	0.00	0.00	0.00
80%	0.22	0.15	0.11	0.08	0.06	0.06	0.05	0.03	0.03	0.02
90%	0.43	0.32	0.28	0.25	0.22	0.21	0.19	0.18	0.16	0.14
100%	0.63	0.54	0.52	0.50	0.48	0.48	0.46	0.45	0.44	0.43
110%	0.78	0.72	0.71	0.70	0.70	0.70	0.70	0.70	0.69	0.68

Table 6. Kobe II Strategy Matrix for blue marlin in the Indian Ocean obtained from selected scenario (S10). Probability (percentage) of achieving the green quadrant of the Kobe plot under the constant catch with 10-110% of the 2020 catch level (7,126 t) for 10 years projection.

Catch	2021	2022	2023	2024	2025	2026	2027	2028	2029	2030
10%	0.34	0.77	0.99	1.00	1.00	1.00	1.00	1.00	1.00	1.00
20%	0.34	0.73	0.96	1.00	1.00	1.00	1.00	1.00	1.00	1.00
30%	0.34	0.68	0.93	1.00	1.00	1.00	1.00	1.00	1.00	1.00
40%	0.34	0.62	0.88	0.97	1.00	1.00	1.00	1.00	1.00	1.00
50%	0.34	0.56	0.80	0.94	0.99	1.00	1.00	1.00	1.00	1.00
60%	0.34	0.50	0.71	0.86	0.95	0.98	1.00	1.00	1.00	1.00
70%	0.33	0.44	0.61	0.76	0.86	0.93	0.96	0.98	0.99	1.00
80%	0.31	0.37	0.49	0.61	0.71	0.79	0.85	0.89	0.92	0.94
90%	0.27	0.29	0.35	0.44	0.52	0.58	0.63	0.68	0.71	0.76
100%	0.21	0.21	0.24	0.29	0.32	0.36	0.39	0.41	0.45	0.49
110%	0.14	0.13	0.14	0.18	0.19	0.21	0.22	0.25	0.28	0.24